1974AREPS...2..333B

Copyright 1974. All rights reserved

THE ATMOSPHERE OF MARS

* 10026

Charles A. Barth

Department of Astro-Geophysics and Laboratory for Atmospheric and Space Physics, University of Colorado, Boulder, Colorado 80302

INTRODUCTION

Our knowledge of the Mars atmosphere has increased rapidly during the past several years because of intensive spacecraft exploration of that planet and because of earth-based observations using improved spectroscopic techniques. The atmosphere of Mars is essentially a pure carbon dioxide atmosphere that contains a small and seasonally varying amount of water vapor. Observations have revealed a number of minor constituents that arise from the interaction of solar radiation with water vapor and carbon dioxide: namely, carbon monoxide, atomic oxygen, molecular oxygen, ozone, and atomic hydrogen. At the surface of Mars the atmospheric pressure is less than one hundredth of the pressure at the surface of the earth and, in fact, corresponds in magnitude to the pressure in the earth's stratosphere. Near the surface the temperature of the atmosphere is low and decreases further with increasing height and reaches the condensation temperature of carbon dioxide under many circumstances. Elevation differences on Mars are large and, consequently, there are large variations in the surface pressure around the planet. Because of the thinness of the atmosphere, the temperature varies greatly from day to night. Winds blow and at times blow very intensely. Dust storms are created by the winds and on rare occasions envelope the entire planet. Dust in the atmosphere absorbs heat and changes the temperature structure of the atmosphere, even when present in small amounts. Frozen carbon dioxide is the major constituent of the polar caps, but the caps also contain water ice, perhaps even in large amounts. The amount of water vapor in the atmosphere appears to be controlled, in part, by seasonal conditions at the polar caps and also by the temperature of the surface at all locations on Mars. Extensive cloud systems appear on Mars and perhaps all those that have been observed are composed of water ice crystals. The amount of ozone in the atmosphere varies seasonally and from day to day. It appears that when ozone is present, water vapor is not; and when water vapor is present, ozone disappears. In the upper atmosphere the temperature is low, but not low enough to prevent the escape of atomic hydrogen through thermal evaporation. The ionosphere of Mars is composed of ions that result from the photochemistry of the carbon dioxide–water vapor atmosphere. Recombination

© Annual Reviews Inc. • Provided by the NASA Astrophysics Data System

1974AREPS...2..333B

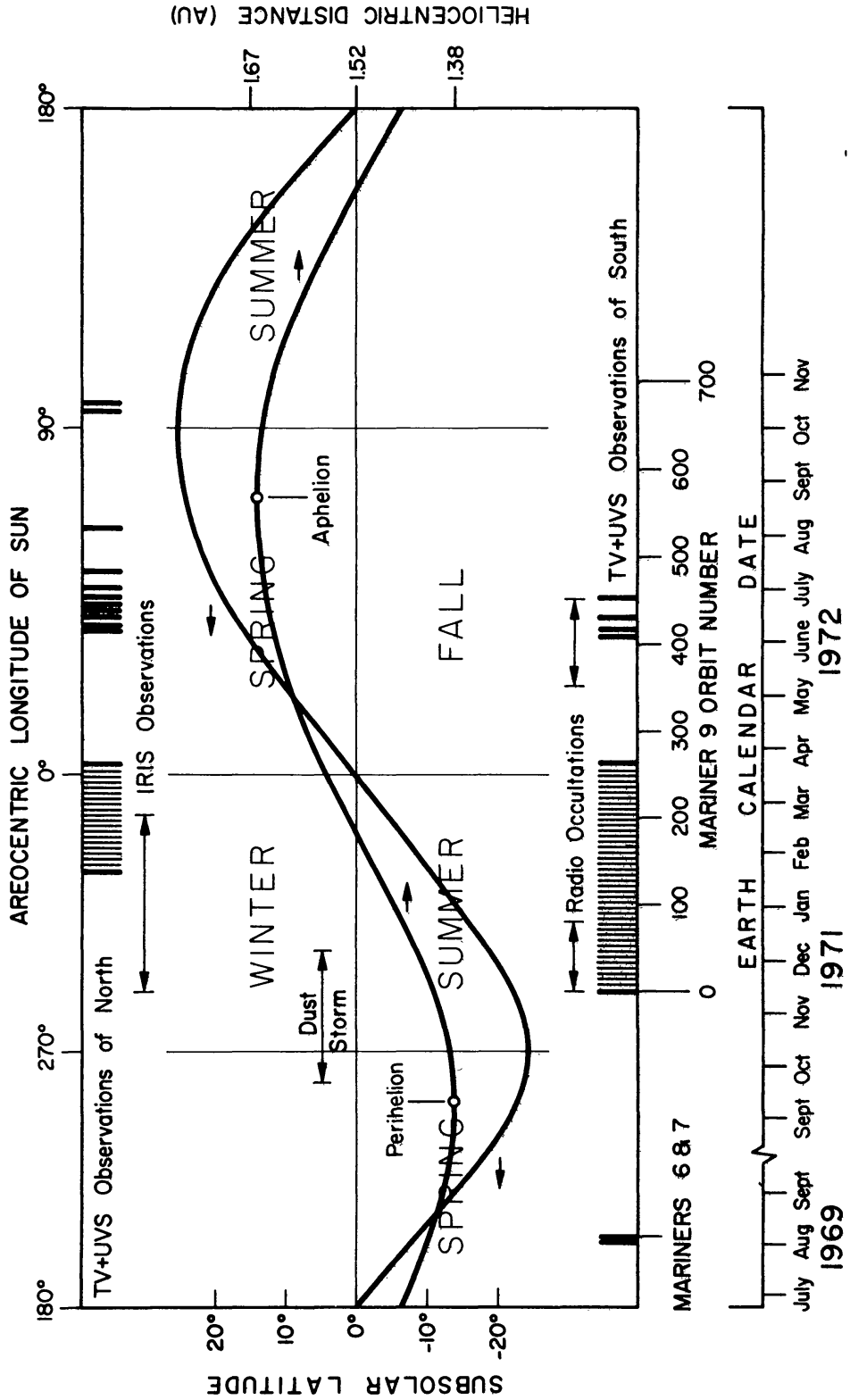

Figure 1 A Mars seasonal calendar. The dates of Mariner observations are shown related to the Mars local season.

© Annual Reviews Inc. • Provided by the NASA Astrophysics Data System

1974AREPS...2..333B

of these ions provides nonthermal mechanisms for atoms to escape from the upper atmosphere of Mars. Since the pressure and even the composition of the Mars atmosphere is intimately connected to the temperature of polar caps, long-term changes in the heat input to the polar caps may lead to dramatic changes in the pressure and temperature of the atmosphere and even to the amount of water on the surface of the planet.

SPACECRAFT OBSERVATIONS

Observations of Mars from planetary spacecraft began in July of 1965 with the Mariner 4 "fly-by" mission and continued in July and August of 1969 with two additional fly-by missions, Mariner 6 and 7. In 1971 and 1972, extensive planetary observations were conducted with three spacecraft in orbit about Mars: Mariner 9 operating from November 1971 until October 1972, and Mars 2 and 3 observing between December 1971 and March 1972. In comparing observations from the different spacecraft missions to each other and to earth-based observations, it is appropriate to take into account the season on Mars at the time. In particular, Mariner 9 operated in Mars orbit for almost half of a Mars year and acquired measurements during all four seasons while observing both the northern and southern hemispheres. Figure 1 indicates the seasonal time of the Mariner 9 observations and it may be used to interrelate other observations as well. Since on Mars the seasons are produced by the inclination of the spin axis to the orbital plane—the obliquity—and by the eccentricity of the orbit, both properties are plotted in Figure 1. Mariner 9 began observations in the southern hemisphere where it was early summer, shortly after going into orbit. Later in the mission when observations were begun in the north polar region, it was past mid-winter. All observations stopped shortly after the beginning of the spring-fall seasons with resumption in mid-fall in the north. A few observations were made at the beginning of summer in the north polar region. The equatorial region and the south polar region during early spring were observed from Mariner 6 and 7; Mariner 4 flew by Mars during the late summer-winter season. The Mars 2 and 3 observational period was from mid to late summer-winter. Several Soviet Mars spacecraft are scheduled to arrive at Mars in 1974, near the beginning of the spring-fall season.

COMPOSITION

The atmosphere of Mars is essentially a pure carbon dioxide atmosphere. The evidence for this has accumulated from observations made from spacecraft and from earth-based telescopes. The first direct measurement of the Mars atmosphere, made by the Mariner 4 radio occultation experiment in July 1965, showed that the total atmospheric pressure was small, somewhere between 4.1 and 6.2 mbar (41).

Since this experiment measures the index of refraction of the atmosphere, a knowledge of the atmospheric composition is necessary to determine a unique value for the pressure. However, when the radio occultation results are combined

© Annual Reviews Inc. • Provided by the NASA Astrophysics Data System

1974AREPS...2..333B

with spectroscopic measurements of the carbon dioxide abundance, useful constraints are placed upon the composition of the Mars atmosphere. High resolution spectroscopy of the 1.038 and 1.050 μ bands in the Mars atmosphere from an earth-based telescope during the 1967 opposition showed that the amount of CO_2 in the Mars atmosphere was 78 ± 11 m-atm,[1] an amount corresponding to a partial pressure between 4.7 and 6.3 mbar (14). With the caution that the two observations—the radio occultation and the high resolution spectrocopy—were made at different locations on the planet and at different times, the results may be combined to show that the Mars atmosphere must contain at least 75% carbon dioxide.

At the time of the 1967 opposition of Mars, high resolution spectra were obtained in the near-infrared using the technique of Fourier spectroscopy (18). This was a significant advance in earth-based planetary spectroscopy. Analysis of these observations showed that all of the features in the Mars spectrum are produced by carbon dioxide and carbon monoxide in the Mars atmosphere (39). A detailed analysis of the high resolution Mars spectra yielded both the total pressure of the Mars atmosphere and the partial pressure of carbon dioxide (93). Within the errors of the analysis, the partial pressure of CO_2 was found to be equal to the total pressure of 5.2 ± 0.3 mbar (abundance 70 ± 4 m-atm). An analysis of the 2.35 μ CO band showed an abundance of carbon monoxide of 13 ± 8 cm-atm (94) showing that the percentage composition of carbon monoxide in the Mars atmosphere is only 0.2% (limits 0.07–0.32%). Some implications of this small ratio will be discussed later.

Water vapor in the Mars atmosphere is measurable with earth-based telescopes using high resolution spectroscopy in the near infrared portion of the spectrum (8200 Å water vapor band) (86). Telescopic observations show that the amount of water is variable, ranging from the detection limit of about 10 μm precipitable water to nearly 60 μm, depending upon the season (4). During the summer season in either hemisphere, maximal amounts of water vapor are found. Following the equinoxes, the amount of water vapor in the Mars atmosphere has been below the detection limit of earth-based telescopes.

The Mariner 6 and 7 infrared spectrometer observations of Mars during the 1969 fly-by detected only three gaseous constituents: carbon dioxide (71 m-atm), carbon monoxide, and water vapor (37). Although these spectrometers had the sensitivity and resolution to detect parts per million of a number of molecules, no additional constituents were found. No ammonia, no nitrogen dioxide, and no nitric oxide were detected with an instrument sensitivity of less than a part in a million. With a sensitivity of a few parts in a million, the following hydrocarbons were also absent: methane, ethane, ethylene, and acetylene. A compilation of upper limits of minor constituents is given in Table 1. The low limits determined by the

[1] The amount of the atmospheric constituent is expressed in meter-atmospheres, the thickness of the column in meters when compressed to standard temperature and pressure on the earth; 1 m-atm $= 2.69 \times 10^{21}$ molecules per square centimeter, 1 cm-atm $= 2.69 \times 10^{19}$ molecules per square centimeter, 1 μm-atm $= 2.69 \times 10^{15}$ molecules per square centimeter.

© Annual Reviews Inc. • Provided by the NASA Astrophysics Data System

1974AREPS...2..333B

Table 1 Upper limits for minor constituents

	Molecule	Abundance
Mariner 6 and 7		(μm-atm)
Infrared spectrometer	NO_2	16
(curve of growth) (37)	NH_3	31
	C_3O_2	32
	SO_2	37
	OCS	40
	NO	50
	CH_4	260
	N_2O	1300
Mariner 6 and 7		(mm-atm)
Infrared spectrometer	C_2H_4	0.12
(absorption coefficient) (37)	CS_2	0.14
	C_2H_6	0.25
	C_6H_6	0.40
	C_2H_2	0.64
	HCN	0.96
Earth-based		(μm-atm)
Infrared interferometer (13)	HCl	11
	HCOH	50
	HCOOH	70
OAO		(μm-atm)
Ultraviolet spectrometer (72)	SO_2	10
	H_2S	10
	NH_3	10
	NO_2	10
	N_2O_4	30

Mariner 6 and 7 infrared spectrometer experiment were the result of an elaborate laboratory program (37).

Additional earth-based infrared observations of Mars, made during the 1969 opposition using a Connes-type interferometer (13) were specifically designed to search for hydrochloric acid, which had been discovered on Venus with the same type instrument. A search was also made for formaldehyde and formic acid in the atmosphere of Mars. None of these constituents were found with the detectability limit one part per million or better. The upper limits for these molecules are listed in Table 1.

During the 1971 opposition of Mars, earth-based high resolution spectroscopic observations led to the discovery of molecular oxygen in the atmosphere of Mars (3, 17). Two rotational lines in the A-band of molecular oxygen at 7635 Å were observed at a time when the Doppler shift permitted them to be distinguished

© Annual Reviews Inc. • Provided by the NASA Astrophysics Data System

1974AREPS...2..333B

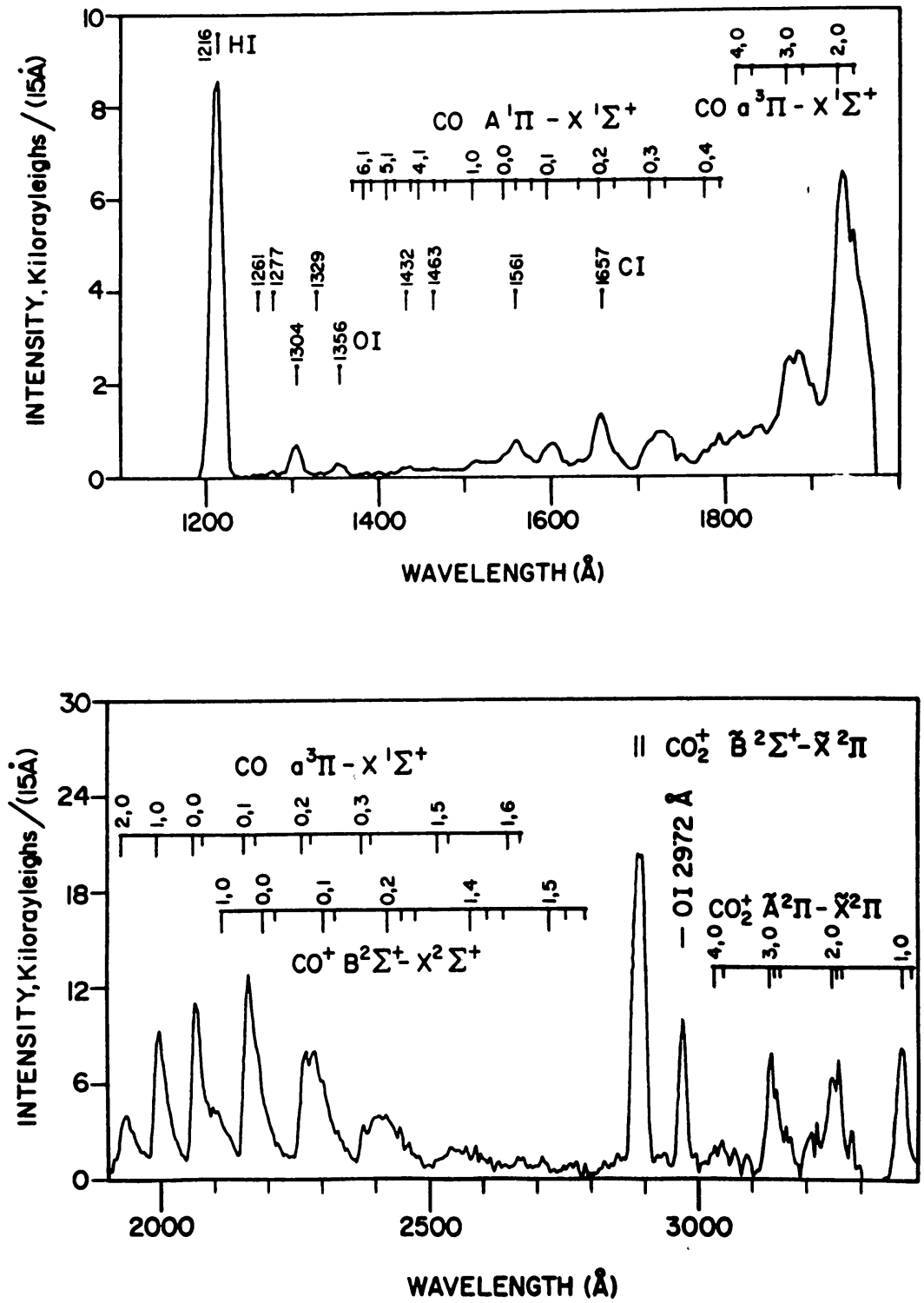

Figure 2 Mars airglow spectrum between 1100 Å and 3400 Å obtained by the ultraviolet spectrometer on Mariner 9 (9).

© Annual Reviews Inc. • Provided by the NASA Astrophysics Data System

1974AREPS...2..333B

from the earth's molecular oxygen. The amount of oxygen observed was small, 10.4 ± 1.0 cm-atm, corresponding to a percentage composition of 0.13%.

The Mariner 6 and 7 ultraviolet spectrometer experiment measured the emission spectrum of the upper atmosphere of Mars (6). Ultraviolet observations show Mars has an essentially pure carbon dioxide atmosphere. With two exceptions, all of the observed spectral features can be explained by the direct or indirect action of solar ultraviolet radiation on carbon dioxide (7). The two exceptions are resonance lines of atomic hydrogen at 1216 Å and atomic oxygen at 1304 Å. The atomic hydrogen and atomic oxygen in the Mars atmosphere are produced by the photodissociation of water vapor and carbon dioxide. A radiative transfer treatment of the atomic hydrogen Lyman alpha 1216 Å data shows the amount of atomic hydrogen at the top of the Mars atmosphere (250 km) is 3×10^4 atoms cm^{-3} (2). An elaborate analysis of the atomic oxygen 1304 Å data concludes that the concentration of atomic oxygen in the upper atmosphere at 135 km lies between 0.5 and 1% of the total density at that altitude (90). Molecular nitrogen was searched for in the ultraviolet data and not found (6). The sensitivity of the ultraviolet spectrometer for detecting molecular nitrogen is estimated to be approximately 1% (5). A comparison of the ultraviolet data with calculations based on a number of model atmospheres leads to estimates of the nitrogen to carbon dioxide mixing ratio that lie between 0.5 and 5%, depending on the degree of mixing in the atmosphere (22).

Hundreds of ultraviolet spectra were obtained of the Mars upper atmosphere during the long operational lifetime of the Mariner 9 Mars orbiter. The Mars airglow spectrum in Figure 2 is the sum of a large number of individual observations (9). This spectrum, with higher signal to noise ratio than the Mariner 6 and 7 data, shows all of the spectral features first identified in the 1969 experiment and no others. Atomic hydrogen and atomic oxygen were also measured by the ultraviolet photometer on Mars 3 (23, 47).

Ozone was first detected on Mars by the Mariner 7 ultraviolet spectrometer (8) and has been measured extensively from the Mariner 9 orbiter. Figure 3 shows the

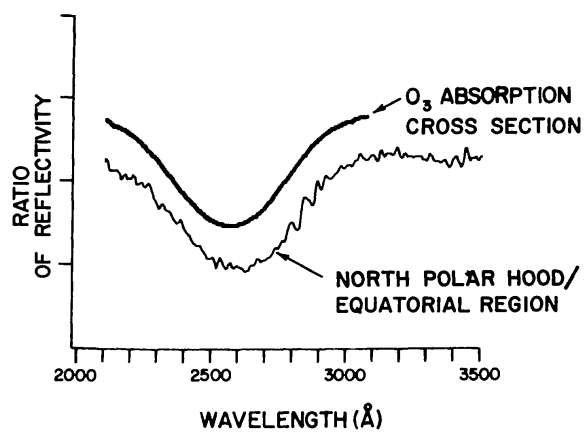

Figure 3 Mars absorption spectrum compared with laboratory ozone curve (48).

© Annual Reviews Inc. • Provided by the NASA Astrophysics Data System

1974AREPS...2..333B

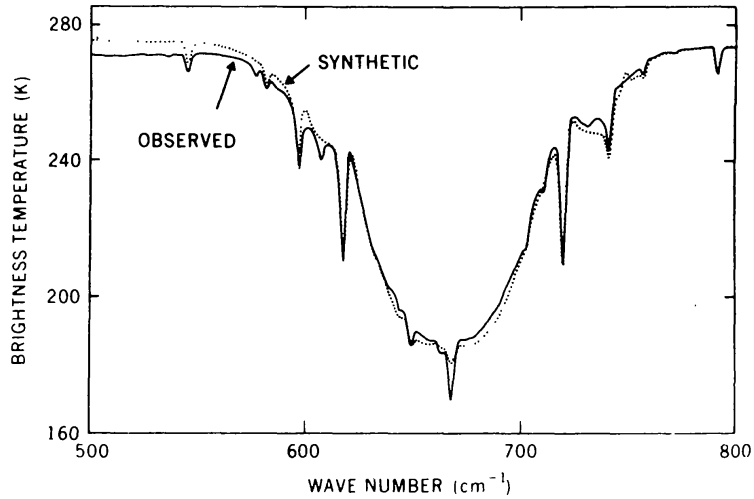

Figure 4 Mars absorption spectrum in the 12.5 to 20 μ region measured by the infrared interferometer spectrometer experiment on Mariner 9 compared to carbon dioxide synthetic spectrum (19).

distinctive spectral absorption feature in the 2000 to 3000 Å wavelength region that is used to detect and measure ozone (48). The amount present in the atmosphere is small and variable. Over most of the planet, the amount is less than the detection limit of 3 μm-atm or less than 0.5 parts in 10 million. In the polar regions, detectable amounts occur varying from 3 μm-atm to 60 μm-atm (10). The seasonal variation and correlation with other properties of the Mars atmosphere will be discussed in a subsequent section.

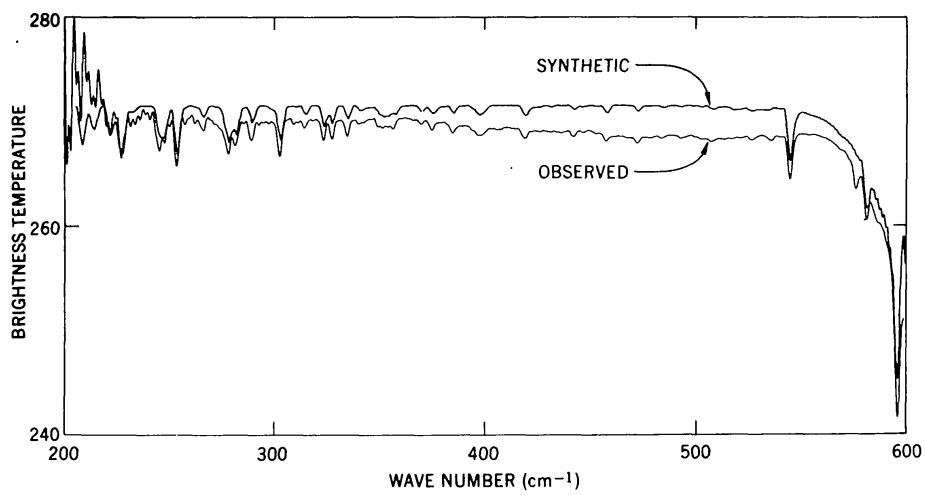

Figure 5 Mars absorption spectrum in the 16.7 to 50 μ region observed by Mariner 9 infrared interferometer spectrometer compared to water vapor synthetic spectrum (19).

© Annual Reviews Inc. • Provided by the NASA Astrophysics Data System

1974AREPS...2..333B

The Mariner 9 infrared interferometer spectrometer obtained many tens of thousands of spectra of Mars in the wavelength region 5 to 50 μ (200 to 2000 cm^{-1}). The thermal emission of the surface and atmosphere of Mars was observed over a number of different Mars environmental conditions; for example, the planetwide dust storm, the subsequent clear atmosphere, the receding polar cap, and the changing polar hood. The only spectral features observed by this instrument were those produced by carbon dioxide (including its isotopes), by water vapor, and by the atmospheric dust. No other molecules were observed (33). In the wavelength region observed, the most prominent CO_2 spectral feature is the fundamental 15 μ band. Figure 4 shows this observed band and numerous other CO_2 bands as well, including the isotopes $O^{16}C^{13}O^{16}$, $O^{16}C^{13}O^{18}$, and $O^{16}C^{12}O^{18}$. The isotopic ratios for C^{12}/C^{13} and O^{16}/O^{18} are in general agreement with ratios found on earth (19). Figure 5 shows the spectral absorption produced by 10 μm of precipitable water in the Mars atmosphere. The amount of water is variable and depends on the location and season. This seasonal variation will be discussed in a subsequent section.

STRUCTURE OF THE LOWER ATMOSPHERE

Following the first direct measurement of the structure of the lower atmosphere of Mars by Mariner 4 in 1965 (41), the radio occultation experiments on Mariner 6 and 7 again probed the atmosphere in 1969. Temperature profiles from the four 1969 measurements, which included locations ranging from equatorial to polar latitudes, are shown in Figure 6 (42, 43, 75). The temperature of the atmosphere

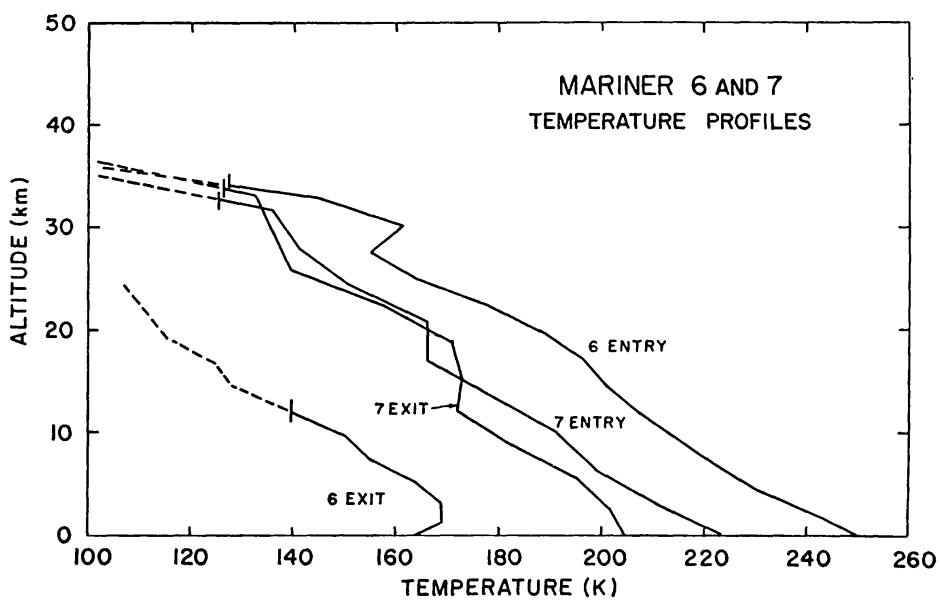

Figure 6 Atmospheric temperature profiles for the four occultation points of Mariner 6 and 7(75). (Figure reproduced by permission of *J. Atmos. Sci.*)

© Annual Reviews Inc. • Provided by the NASA Astrophysics Data System

1974AREPS...2..333B

was 250°K at the warmest location (afternoon near the equator) and 170°K at the coldest location (before midnight in the north polar region). With increasing altitude, the temperature dropped with a lapse rate of about 3°K/km for the nonpolar measurements. For the north polar region, the atmospheric temperature at 12 km altitude decreased to a value of 140°K. Above this altitude, the atmosphere was cold enough for carbon dioxide, the major constituent of the atmosphere to condense. Observations by the Mariner 6 and 7 infrared spectrometer of the 4.3 μ "reflection-absorption" band of solid carbon dioxide have been interpreted as direct evidence for the presence of solid carbon dioxide in the atmosphere of Mars (34a).

At the six locations probed by the Mariner 4, 6, and 7 radio occultation experiments, the measured values of the surface pressure varied from 4.2 to 7.3 mbar. The variations are real, due to variations in elevation at the different locations. On earth, pressures of this magnitude are reached in the stratosphere at an altitude of about 33 km.

In 1971 and 1972, measurements of the Mars lower atmosphere were made by the Mariner 9 radio occultation experiment during two periods: first, during mid-summer in the southern hemisphere (mid-winter in the north), while a planetwide dust storm was in progress; second, during spring in the northern hemisphere (fall in the south) while the atmosphere was relatively clear (see Figure 1). Measurements during the first period were in two groups: daytime measurements between latitudes 40°S and 20°N and nighttime (or twilight) measurements near 65°N. During the first nine orbits of Mariner 9, the atmosphere was isothermal in the 40°S to 20°N latitude band in the lowest 10 km (44). Throughout the first 40 days (80 orbits), while occultation measurements were possible, the magnitude of the temperature gradient gradually increased and at the same time, the temperature of the atmosphere directly above the surface increased (45). However, the lapse rate varied from measurement to measurement, and the systematic increase apparently reversed toward the end of this period. The magnitude of the mean lapse rate was always less than 2.5°K/km.

Measurements made at night or in the early morning in the 65°N latitude band showed that the atmospheric temperature reached the condensation temperature of carbon dioxide at an altitude of 10 km or lower (45). The season at this time was mid-winter, when the carbon dioxide polar cap was forming beneath the polar hood.

During the second period that Mariner 9 radio occultation measurements were possible, essentially all latitudes were sampled, including both polar regions. At this time, the atmosphere was clear; the planetwide dust storm had subsided four months earlier. Measurements at equatorial and mid-latitudes showed that the atmosphere was no longer isothermal. The temperature did decrease with increasing altitude, but the lapse rate surprisingly had a mean value of only 2.3°K/km, still less than the mean lapse rate of the few measurements by Mariner 6 and 7 (46).

Over the north polar cap in mid-spring, the radio occultation experiment measured atmospheric temperatures between 178 and 191°K on different days; all temperatures above the sublimation temperature of carbon dioxide (147°K at 6.105 mbar). The lapse rate was 2.2°K/km. Measurements of pressure in the north

© Annual Reviews Inc. • Provided by the NASA Astrophysics Data System

1974AREPS...2..333B

polar region showed values between 4.4 and 7.4 mbar, due to elevation differences, with a mean pressure of 5.7 mbar. The south polar cap has a mean elevation of 3 to 4 km higher than the north polar cap. The temperature of the atmosphere above the south polar cap (season mid-fall) was consistent with temperatures necessary for carbon dioxide condensation (46).

Approximately 222 individual radio occultation measurements were made by Mariner 9. Because of elevation differences, the pressure at the surface varied for all of these observations. At the lowest elevation, in the 65°N latitude band, the pressure was over 10 mbar (46). Near the top of Middle Spot, the highest elevation measured by the radio occultation experiment, the pressure was 1 mbar. The mean of all of the pressures measured by the radio occultation experiment was 6.6 mbar.

Temperature profiles of the lower atmosphere of Mars were obtained by the Mariner 9 infrared interferometer spectrometer experiment. Analysis of the spectral shape of the 667 cm^{-1} (15 μ) carbon dioxide band leads to the determination of the temperature at a number of discrete pressure levels in the altitude range from the surface to 40 km. Over 17,000 temperature profiles were measured during the first 210 orbits of Mariner 9, a period which lasted from early summer to late summer in the southern hemisphere (early winter to late winter in the north). This period included the abatement of the planetwide dust storm and the clearing of the atmosphere. From this vast resource of data, examples of a number of the important results have been reported (19, 32, 33).

Changes in the temperature structure of the atmosphere at mid-latitudes are illustrated in Figure 7. Early in summer, during the dust storm (Revolution 20), the atmosphere was relatively warm from the surface all the way up to 40 km and the temperature gradient in the lowest 10 km was small. At mid-summer, when the dust storm was beginning to subside, the atmosphere above 10 km began to cool. Below the 10 km level, the atmosphere warmed up and a temperature gradient of −3°K/km was established from the surface up to 20 km. Above that altitude, the

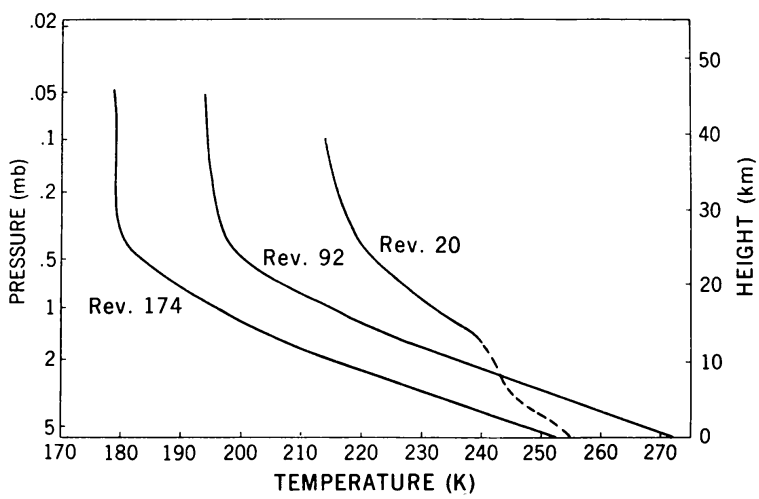

Figure 7 Atmospheric temperature profiles for three orbits during the Mariner 9 mission, showing changes detected for differing atmospheric conditions (33).

© Annual Reviews Inc. • Provided by the NASA Astrophysics Data System

1974AREPS...2..333B

atmosphere became isothermal. Later in the summer when the atmosphere was essentially clear, the temperature dropped further and the temperature gradient remained near −3°K/km (33).

Temperatures over the south polar region were measured by the infrared interferometer spectrometer during the summer and over the north polar region during the winter and spring. Temperature profiles over the south polar region for three dates in summer are shown in the lefthand side of Figure 8. Early in summer (Rev 30), the temperature structure was relatively warm and nearly isothermal. In mid-summer (Rev 116), the temperature dropped and a temperature inversion appeared with a maximum near the 2 mbar (10 km) level. At the end of summer (Rev 188), the temperature dropped still further. Above the 0.5 mbar (25 km) level, the temperature was isothermal at about 155°K. In all three of these cases, the atmospheric temperature was greater than the surface temperature. Over the north polar region in mid-winter (Rev 102), the temperature of the atmosphere was higher above 25 km than at lower altitudes (righthand side of Figure 8). Below the 3 mbar (7 km) level, the temperature was approximately 150°K, just above the condensation temperature of carbon dioxide. The winter temperature of the polar cap was 145°K, the condensation temperature of dry ice. In late spring (Rev 528), the temperature of the atmosphere directly above the polar cap rose, leading to a negative

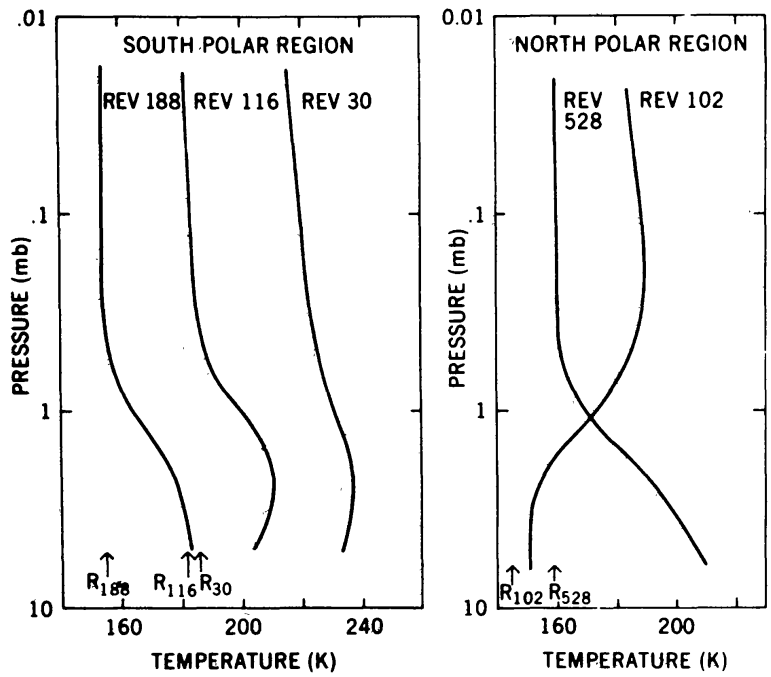

Figure 8 Atmospheric temperature profiles for the south polar cap region in summer and for the north polar cap during winter and spring. These profiles were obtained by the infrared spectrometer on Mariner 9. The arrows near the bottom of the figure indicate the surface temperatures (19).

© Annual Reviews Inc. • Provided by the NASA Astrophysics Data System

1974AREPS...2..333B

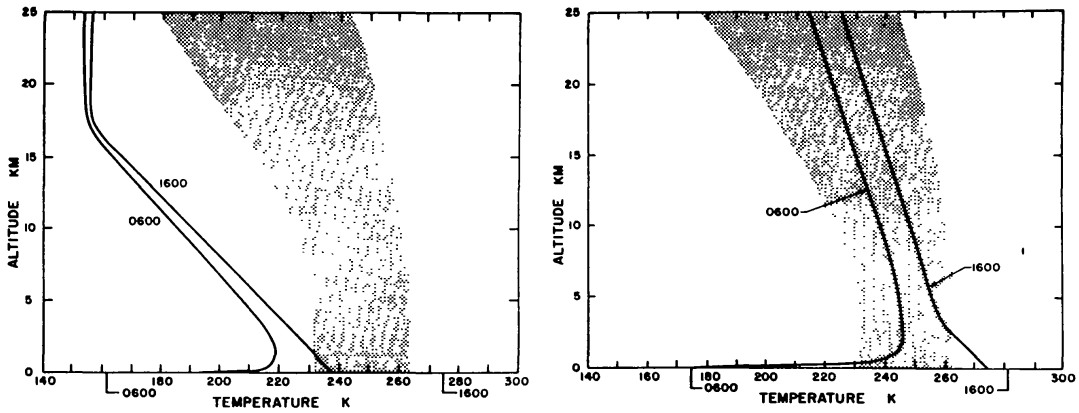

Figure 9 Theoretical and observed temperature profiles for Mars. The stippled areas include the Mariner 6 and 7 observations: the theoretical profiles are for a pure CO_2 atmosphere (left) and an atmosphere containing dust (right) (28). (Figure reproduced by permission of *J. Atmos. Sci.*)

temperature gradient. The atmosphere was isothermal with a temperature of 160°K above the 0.5 mbar (25 km) level.

Theoretical calculations of the temperature structure of the Mars lower atmosphere predict a lapse rate of 5°K/km for a clear carbon dioxide atmosphere under conditions of radiative-convective equilibrium (27). Mariner 6 and 7 and the extensive Mariner 9 measurements of the temperature profile showed the lapse rate to be less than this value when the atmosphere was clear and much less when the atmosphere was dusty. When dust is suspended in the atmosphere, theoretical calculations show that the dust heats the atmosphere while absorbing solar radiation (28). Even a very small amount of dust causes the lapse rate to be less than the value calculated for a clear atmosphere. Large amounts of dust cause the atmosphere to become very stable and nearly isothermal from the surface to an altitude of 25 km. The dusty atmosphere is much hotter than the clear atmosphere. These results are illustrated in Figure 9 (28). Inclusion of large-scale dynamics into the calculation of the temperature profile of the Mars atmosphere also causes the calculated lapse rate to be less than the value calculated considering only radiation and convection (15, 49a, 89).

VARIATIONS IN THE LOWER ATMOSPHERE

Variations occurring in the atmosphere of Mars can be separated into diurnal and seasonal changes. Superimposed on the regular changes are unexpected events that characterize Mars weather. Mars rotates at a rate slightly slower than the earth: the day is 24 hr and 39 min long. While the Mars year is almost twice as long as the earth's, the Mars obliquity of 25° produces seasons similar to those on earth. However, on Mars at the present time the greater eccentricity of the orbit accentuates the seasons in the southern hemisphere and moderates them in the north.

Variations in the temperature of the atmosphere as a function of local time and

© Annual Reviews Inc. • Provided by the NASA Astrophysics Data System

1974AREPS...2..333B

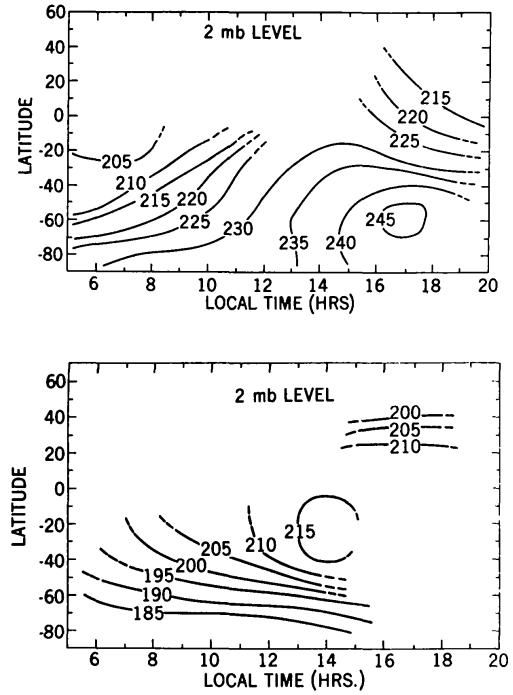

Figure 10 Atmospheric temperature on Mars showing latitude and local time variations. The upper figure is from observations taken during the dust storm, the lower figure is from observations taken when the atmosphere was relatively clear (33).

latitude are illustrated in Figure 10. The diurnal behavior of the atmosphere at the 2 mbar level ($\sim$ 10 km) during the dust storm is shown by the isotherms in the upper part of the figure. The temperature maximum occurs late in the day, about 5 PM local time, and it lies far south of the subsolar latitude of 20°S. The diurnal behavior of the clear atmosphere is illustrated in the lower part of the figure. The isotherms now show the temperature maximum further north and occurring earlier in the day, about 2 PM local time. The subsolar point at this time was 8°S. Also, the clear atmosphere at the 2 mbar level was cooler than the dusty atmosphere during the storm. Diurnal variations in the atmospheric temperature lead to a tidal effect in the pressure distribution. A calculation of the planetwide pressure distribution based on the temperatures measured during the dust storm is shown in Figure 11 (19). The surface pressure is at its lowest value late in the afternoon, at a latitude between the equator and the maximum temperature location (see Figure 10). Regions far from the place of maximum heating have a surface pressure 25% higher than the minimum surface pressure. When similar pressure calculations are performed for the clear atmospheric temperature distribution, the pressure minimum occurs earlier in the day and is closer to the equator in a manner analogous to the change in location of the temperature maxima in Figure 10. Winds that should result from the measured temperature fields and the tidal pressure variation lead to calculated patterns shown in Figure 12 (19). These results, which apply to conditions during

© Annual Reviews Inc. • Provided by the NASA Astrophysics Data System

1974AREPS...2..333B

the dust storm (summer in the southern hemisphere), show strong northeasterly winds north of the equator and strong northwesterly winds south of the equator in the afternoon. The magnitude of the mean meridional flow crossing the equator depends upon the magnitude of the friction between the atmosphere and the surface,

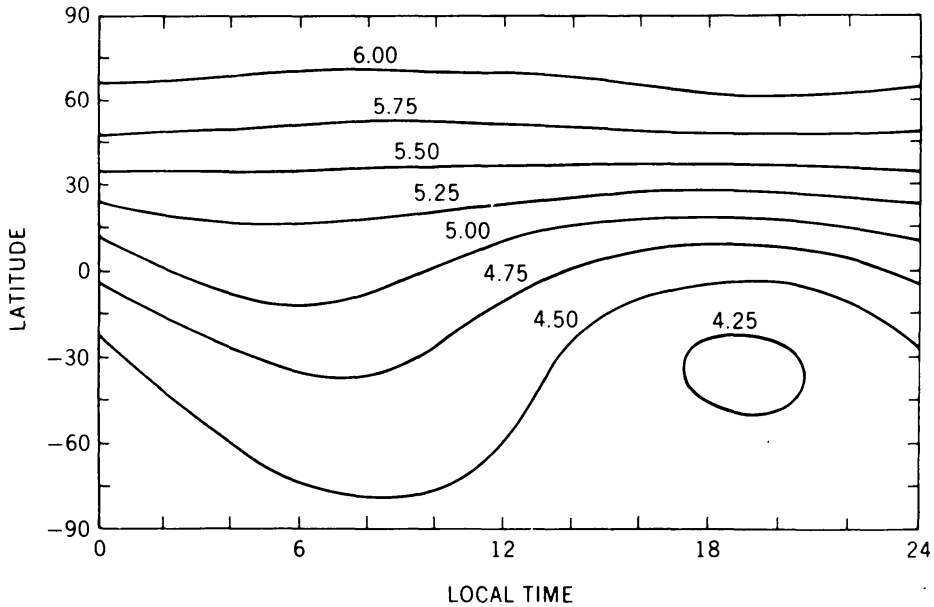

Figure 11 Calculated atmospheric pressure distribution showing tidal effect (19).

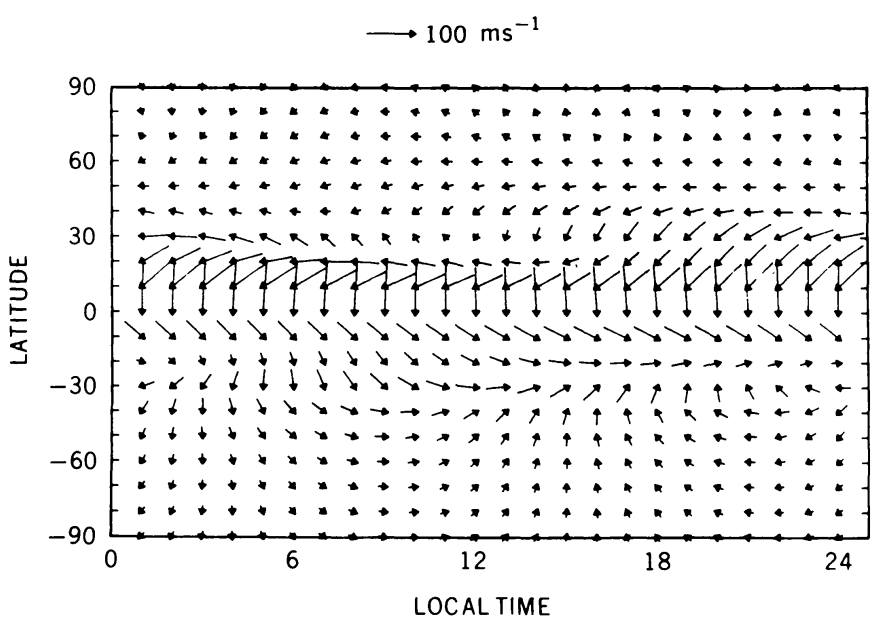

Figure 12 Near surface winds during the great dust storm (19).

© Annual Reviews Inc. • Provided by the NASA Astrophysics Data System

1974AREPS...2..333B

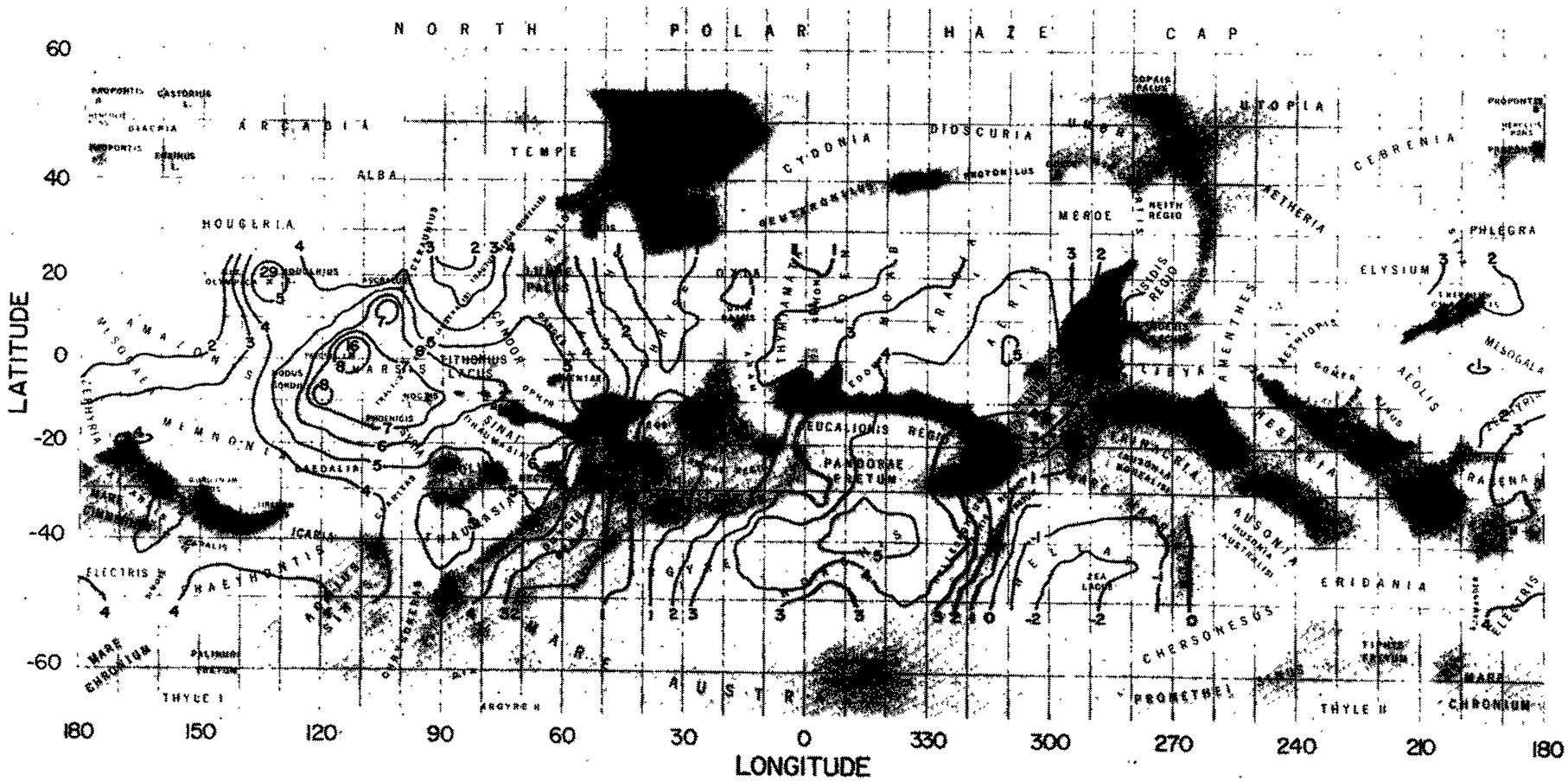

Figure 13 Elevation contours of the surface of Mars measured by the ultraviolet spectrometer experiment (36).

© Annual Reviews Inc. • Provided by the NASA Astrophysics Data System

1974AREPS...2..333B

and is thus highly uncertain (53). These Mariner results confirm the general picture of temperature distributions and wind patterns given by general circulation model calculations (49a).

In the latitude band between 20°N and 20°S, observed wind streak patterns, formed on the surface of Mars from blowing dust, point in directions arising from winds following the calculated patterns (80). At other latitudes, the wind streak patterns do not conform to the calculated wind directions. Topography, an important factor that affects wind patterns, has not been taken into account in the above calculations (27a). On Mars, elevation variations are extreme compared to the scale height of the atmosphere.

In addition to the radio occultation experiment, two other Mariner 9 experiments measured elevation variations on Mars: the infrared interferometer spectrometer (19, 33), and the ultraviolet spectrometer (35, 36). In the lowest measured location on the planet, the Hellas basin, the surface pressure is over 8 mbar, while over the highest large-scale feature, the Tharsis ridge, it is only 3 mbar (19). An elevation contour map based on the ultraviolet spectrometer data, Figure 13, shows an elevation change of over 10 km between these two locations (36). This contour chart also shows that the major high ridges and low depressions are oriented in a north-south direction and, hence, would severely modify the atmospheric winds, particularly those flowing in an easterly or westerly direction.

Seasonal variations of water vapor on Mars were first recorded by spectroscopic observations through earth-based telescopes (81). A summary of earth-based measurements averaged over the disc of Mars is shown in Figure 14. Water vapor is apparently present in the atmosphere in late spring or summer in either hemisphere (4). The maximum amount observed was equivalent to 60 μm of

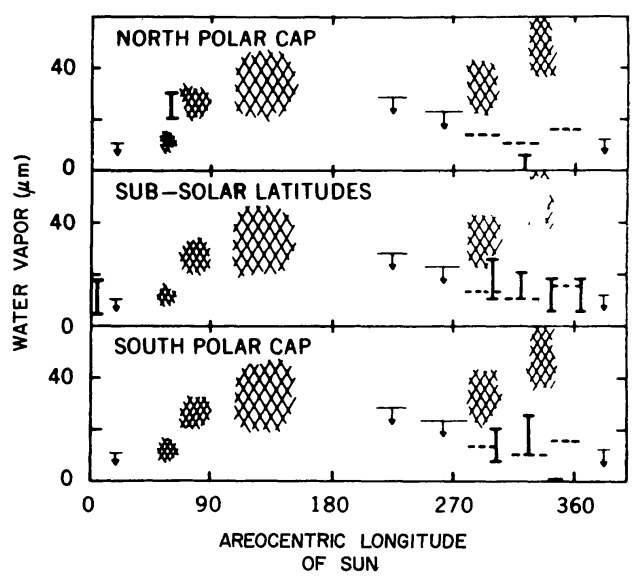

Figure 14 Seasonal variations of water vapor on Mars. Results from earth-based observations are shown with cross hatching, horizontal dash lines, and horizontal lines with arrows (upper limits). Results from Mariner 9 infrared interferometer spectrometer experiment are shown by vertical bars (19).

© Annual Reviews Inc. • Provided by the NASA Astrophysics Data System

1974AREPS...2..333B

precipitable water while the minimum was less than the detection limit of 10 μm. Mariner 9 infrared interferometer spectrometer measurements of water vapor are also included in Figure 14 (19). During summer in the southern hemisphere, between 10 and 20 μm of precipitable water was present over the summer polar region and at subsolar latitudes but water vapor was not detectable over the northern winter polar region. During the northern hemisphere spring, water vapor of between 20 and 30 μm appeared in the atmosphere over the north polar cap and was also observed at subsolar latitudes.

Measurements by the infrared photometer on Mars 3 showed smaller amounts of water vapor in the atmosphere (66). On all observations between December 15, 1971 and February 28, 1972, the maximum amount observed was 3 μm precipitable water. In the polar region, the amount was less than 0.5 μm.

If the sole source of water vapor in the Martian atmosphere were the release of water from subliming carbon dioxide caps, the maximum injection of water vapor into the atmosphere would occur in a relatively short period following the spring equinox when the polar cap begins to recede (51). Measurements by both Mariner 9 and earth-based telescopes show that the seasonal variation is more moderate than expected from a single seasonal injection from the polar caps. Surface temperature measurements of Mars, made by the Mariner 9 infrared radiometer experiment, fall to very low values at night (40). Figure 15 shows surface isotherms calculated from data obtained shortly before the equinox when the atmosphere was clear. At all latitudes, the temperature dropped below 190°K, the condensation temperature of 10 μm of precipitable water. It appears that the observed amount of water in the Mars atmosphere at low and mid-latitudes is equal to the saturation vapor pressure of water at the daily minimum temperature. Water vapor in the atmosphere may exchange with low and mid-latitude permafrost on a daily basis (4).

Ozone is present only in the polar regions of Mars and has a strong seasonal

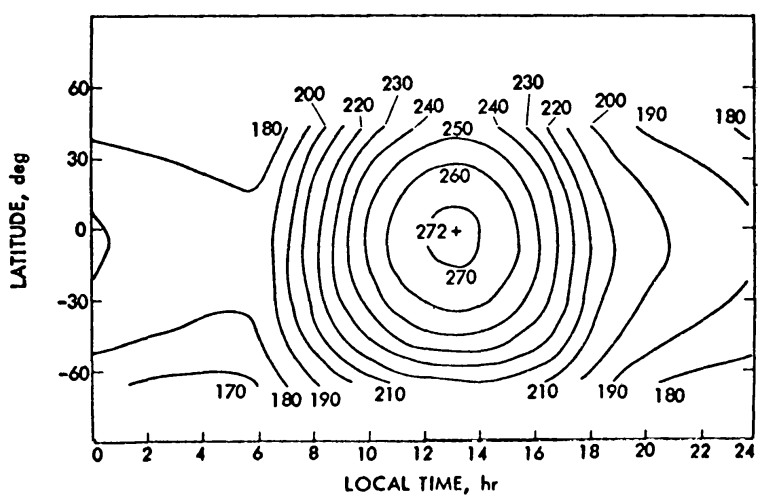

Figure 15 Surface temperatures on Mars calculated for a clear atmosphere based on Mariner 9 infrared radiometer observations (40).

© Annual Reviews Inc. • Provided by the NASA Astrophysics Data System

1974AREPS...2..333B

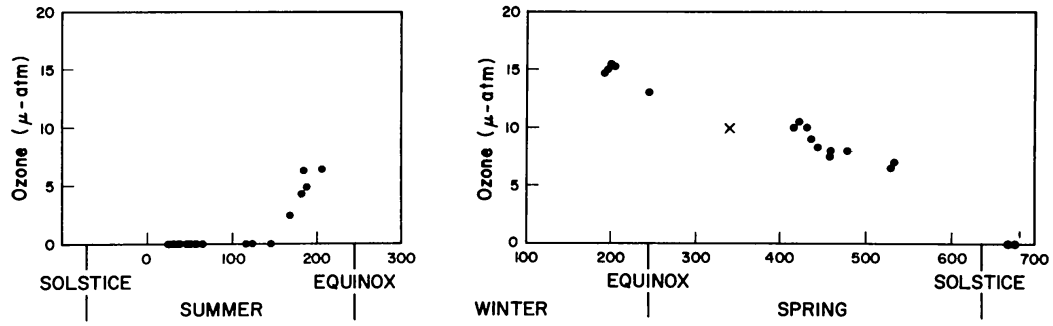

Figure 16 Seasonal ozone over the polar cap of Mars measured by the ultraviolet spectrometer experiments (10). (Copyright 1973 by the American Association for the Advancement of Science.)

variability. Over the polar cap itself, ozone is absent during early and mid-summer. The amount increases during late summer, reaches a maximum in winter, and then decreases in the spring. This behavior is illustrated by the Mariner 9 ultraviolet spectrometer measurements presented in Figure 16 (10). Ozone also appears in the Martian atmosphere in association with the polar hood. In the fall and winter hemisphere, the atmosphere is sufficiently cool so that the entire region poleward of 45° latitude is covered by clouds of water ice crystals. This is the polar hood that has been observed by astronomers for hundreds of years (12). In the latitude range of the hood, ozone actually appears in the atmosphere in late summer, before the polar hood appears. During fall and winter, ozone and the visible hood are both present. Ozone remains in the atmosphere in the spring, after the visible hood has disappeared. The amount of ozone occurring in conjunction with the polar hood is variable, just as the hood itself is variable in its appearance and extent. The conclusion has been drawn that ozone is present when the atmosphere is cold and dry and it disappears, or in fact, never appears, when water vapor is present (11).

During the winter season north of 45° latitude, the Mariner 9 television cameras observed extensive cloud systems (50). This is the location and expected time of appearance of the polar hood, which has been observed from earth-based telescopes for many years (12). In some cases the clouds are diffuse, in other cases there is a distinctive wave-like structure with a spacing of about 5 km. Bands of the wave-like clouds move in the manner of cold fronts on the earth—in one case moving 500 km in a southeasterly direction in one day (50). When these cloud systems flow over topographical features, lee waves are formed in the downwind direction, typically with a spacing of about 30 km. The infrared interferometer spectrometer made atmospheric temperature measurements at the time and place of the occurrence of the cloud systems of the polar hood, and found the temperature is that of water ice crystals (33).

Cloud patterns with wave-like structure were also observed by the Mariner 9 television cameras south of 50° latitude during the fall season (52). From observations both in the southern fall and in the northern winter, the clouds are more diffuse closer to the poles.

© Annual Reviews Inc. • Provided by the NASA Astrophysics Data System

1974AREPS...2..333B

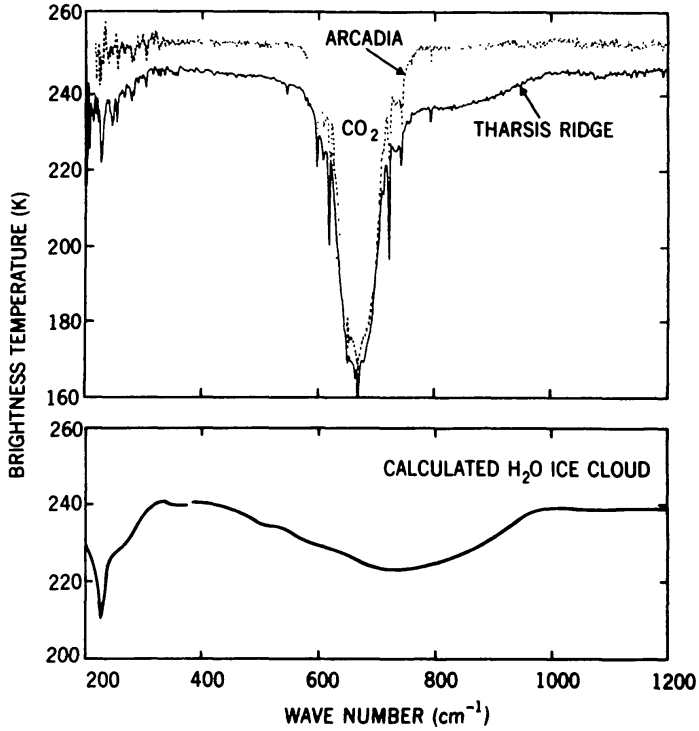

Figure 17 Mars absorption spectrum of water ice clouds over the Tharsis ridge. This spectrum is compared to another Mariner 9 infrared interferometer spectrometer spectrum obtained of a clear atmosphere over the Arcadia region which shows only absorption produced by carbon dioxide and water vapor. A theoretical calculation of the spectrum of a water ice cloud is produced in the lower part of the figure (20). (Copyright 1973 by the American Association for the Advancement of Science.)

Mariner 9 television pictures taken of the Tharsis-Nix Olympica region in late spring and early summer show clouds on the western slopes of the four volcanoes (52). These volcanoes are very high; Nix Olympica rises 25 km above the surrounding terrain (36). Mariner 9 infrared interferometer spectrometer observations of these clouds detected a spectrum characteristic of water ice crystals (20). Figure 17 shows that the spectrum observed over the Tharsis region contains two broad absorption features that are reproduced in a theoretical calculation of the spectrum of a water ice cloud. From earth-based telescopes, clouds in this region of Mars are observed to brighten in the afternoon; they are known as the W-clouds (84). They may be formed by the upslope flow of air from east to west containing perhaps 10 μm of precipitable water. Adiabatic cooling could lead to water ice crystal condensation (74). In addition, convection and even local outgassing might contribute to the cloud formation (52).

During the last few months of 1971, the great planetwide dust storm covered Mars. It began on a high plateau in the southern hemisphere, the Noachis region (see Figure 13), on September 22, 1971, a time when Mars had just passed perihelion and just before summer solstice in the southern hemisphere (see Figure 1) (16). In November, during the first weeks of Mariner 9 observations, the entire planet was

© Annual Reviews Inc. • Provided by the NASA Astrophysics Data System

1974AREPS...2..333B

covered with dust up to an altitude of 50 km (1, 50), except for the south polar region (55).

Theoretical consideration has been given to various aspects of the great dust storm (30, 31, 53). Since a maximum amount of insolation is apparently required to initiate and drive planetwide dust storms, they occur at the time there is a near coincidence between perihelion and southern summer solstice (31). An elevated region such as the Noachis plateau under maximum summer heating would develop a low pressure region with cyclonic flow (30). It has been hypothesized that dust would be raised to substantial heights over an extended area in the region. As dust accumulates in the atmosphere, solar radiation would be directly absorbed, heating the atmosphere still more (28). As more and more energy is absorbed, the dust storm may rotate and grow in a manner analogous to a terrestrial hurricane (30). In addition, the perihelic-summer solstice is a time of sublimation of carbon dioxide from the south polar cap. A large mass outflow from the polar cap could create winds to further drive the dust storm (53).

UPPER ATMOSPHERE AND IONOSPHERE

In the upper atmosphere, above approximately 100 km, the temperature structure is determined in part by heating processes such as photodissociation and photoionization. Two observational techniques utilizing Mariner spacecraft yield direct observational information on the density structure of the upper atmosphere from which temperature profiles can be calculated. On Mariner 4, 6, 7, and 9, the radio occultation experiments measured the electron density directly as a function of altitude (25, 26, 44). Without additional information, however, the interpretation of these data in terms of neutral density and temperature may lead to ambiguous results (25). Ultraviolet spectrometer observations of the Mars airglow from Mariner 6, 7, and 9 yield direct measurements of the rate of photodissociation and photoionization of carbon dioxide as a function of temperature (7). Above the altitude where the maximum rate of photodissociation occurs, the measurement of the intensity variation of the ultraviolet airglow as a function of altitude leads to the determination of the density variation of carbon dioxide. From the scale height (logarithmic variation of density as a function of altitude) the temperature of the atmosphere can be determined. Profiles of the density of carbon dioxide and the temperature as a function of altitude are given in Figure 18 (9). Density distributions for atomic oxygen, carbon monoxide, and molecular oxygen, which are shown in the figure, were calculated assuming diffusive equilibrium above 100 km. This model atmosphere pertains to conditions at the time of the Mariner 6 and 7 observations in 1969. In July and August of 1969, the temperature at the top of the Mars thermosphere, determined from the scale height of the ultraviolet airglow, was 350°K (87), a value far less than anticipated from theoretical calculations (58, 59). In November and December of 1971, the mean thermospheric temperature, determined from Mariner 9 ultraviolet spectrometer measurements of the Cameron bands, was 325°K (88). However, while the mean value of the scale height was 17.8 km, individual values varied from 14.8 km to 24.3 km, corresponding to

© Annual Reviews Inc. • Provided by the NASA Astrophysics Data System

1974AREPS...2..333B

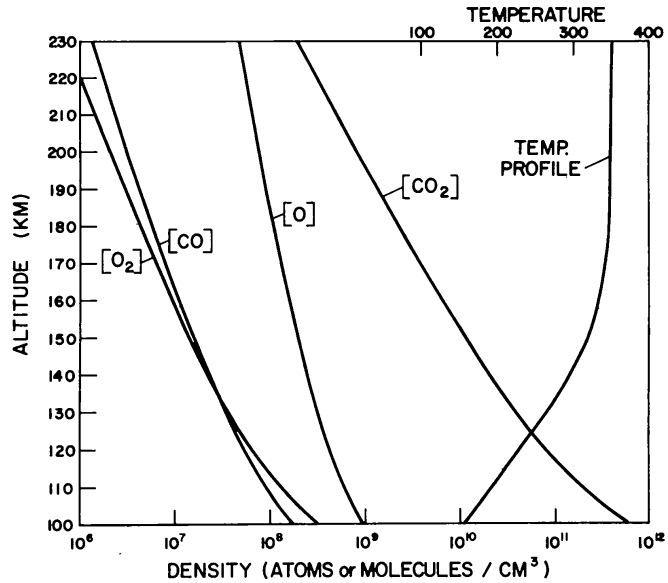

Figure 18 Mars model atmosphere. Density distributions are based on ultraviolet spectrometer, radio occultation and earth-based telescope observations (9).

temperatures of 270 to 445°K. The intensity of the ultraviolet airglow is correlated with an indicator of solar activity, the 10.7 cm solar radio flux; however, the airglow scale height, the measure of temperature, does not appear to correlate with solar activity (88).

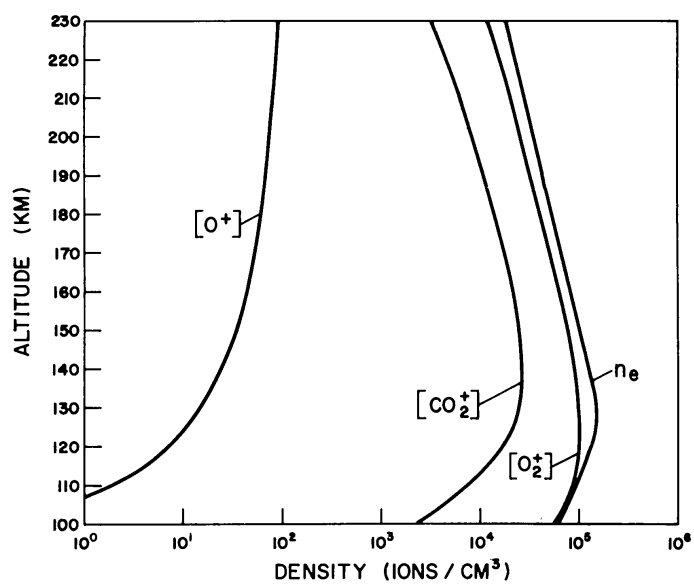

Figure 19 Mars model ionosphere. The model is calculated using radio occultation data together with laboratory measurements of ion chemistry (9).

© Annual Reviews Inc. • Provided by the NASA Astrophysics Data System

1974AREPS...2..333B

Electron density measurements by the Mariner radio occultation experiment may be compared to neutral density measurements by the Mariner ultraviolet spectrometer experiment through the development of an ionospheric theory. Since carbon dioxide is the dominant neutral constituent of the atmosphere, it is not unexpected that it is the major source of ionization in the upper atmosphere. However, carbon dioxide ions are not the most abundant ions in the Mars ionosphere. The ultraviolet airglow does not show the characteristic fluorescence spectrum of carbon dioxide ions, a result first obtained by the Mariner 6 and 7 ultraviolet spectrometers (7) and verified by the more extensive observations of Mariner 9 (9). Laboratory studies have shown that atomic oxygen reacts rapidly with carbon dioxide ions to produce ionized molecular oxygen (24). Theoretical calculations show that, even with the small amounts of atomic oxygen in the Mars upper atmosphere, the most abundant ion in the Mars ionosphere is ionized molecular oxygen (87). A model ionosphere calculated for conditions of photochemical equilibrium is presented in Figure 19 (9). Dissociative recombination of molecular oxygen ions is the major mechanism for loss of ionization. Under the assumption of simple photochemical equilibrium, the scale height of the electron density should be approximately twice the scale height of the major ionizable constituent (87).

Mariner radio occultation experiments measured the scale height and electron density distribution in the Mars atmosphere: once in 1965, twice in 1969, 60 times in 1971, and 25 times in 1972. An altitude profile of the electron density obtained early in the Mariner 9 mission is shown in Figure 20 (45). In 1965, Mariner 4

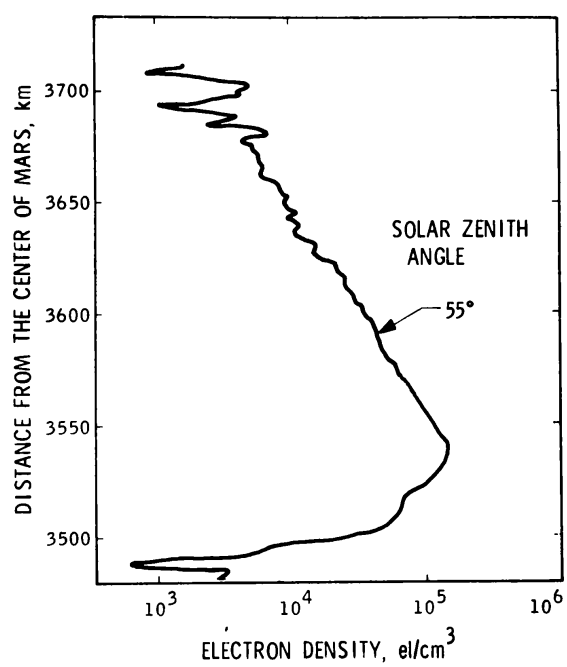

Figure 20 Electron density profile obtained from Mariner 9 radio occultation data (45).

© Annual Reviews Inc. • Provided by the NASA Astrophysics Data System

1974AREPS...2..333B

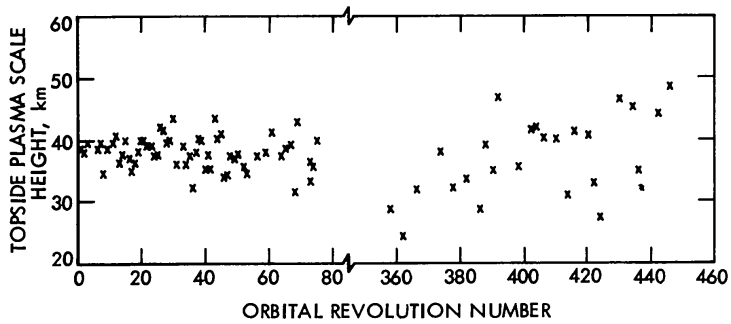

Figure 21 Plasma scale heights from Mariner 9 radio occultation measurements (46).

measured a plasma scale height of 30 km (25); in 1969, Mariner 6 and 7 both measured a plasma scale height of 49 km (26); in 1971 and 1972, Mariner 9 measured a mean scale height of 39 km (45, 46). If the changes in the plasma scale height are solely the result of changes in the temperature of the neutral atmosphere, then assuming simple photochemical equilibrium, the temperatures corresponding to the above scale heights are 270°, 450°, and 350°K, respectively. Individual measurements of the plasma scale height during the Mariner 9 mission are shown in Figure 21 (46). During the first 80 revolutions, the season was summer-winter and a planetwide dust storm existed in the lower atmosphere; between revolutions 360 and 460, the season was spring-fall and the atmosphere was relatively clear (see Figure 1). For these two very different periods, the mean plasma scale height apparently did not change. Daily variations in scale height do not appear to be correlated with indicators of solar activity, such as the 10.7 cm radio flux index (45, 46).

PHOTOCHEMISTRY

During the past several years, there have been a number of papers published on the photochemistry of the Mars atmosphere pertinent to data acquired by planetary spacecraft. The observational findings—the relatively undissociated character of the upper atmosphere and the presence of atomic hydrogen in the Mars exosphere—are related to the photochemistry of both the lower and upper atmosphere. Theoretical studies have dealt with the photochemistry of a dry, carbon dioxide atmosphere (62, 63) and also with the photochemistry of a carbon dioxide atmosphere containing various amounts of water vapor (38, 64, 73).

Photodissociation of carbon dioxide, to produce carbon monoxide and atomic oxygen, takes place from the top of the atmosphere all the way down to the surface (62). In the upper atmosphere, the known recombination reactions are not rapid enough to balance the photoproduction of atomic oxygen to explain the low observed abundances. Eddy diffusion has been proposed as the mechanism for removing atomic oxygen from the upper atmosphere, by transporting it down into the lower atmosphere (83). However, calculations show that the rate of mixing would have to

© Annual Reviews Inc. • Provided by the NASA Astrophysics Data System

1974AREPS...2..333B

be very rapid; the time constant would be 1 hr for a characteristic length of one scale height (63).

Water vapor is photodissociated in the Mars lower atmosphere, mostly in the lowest 10 km (38). The products of this photodissociation are: atomic hydrogen, H; the hydroxyl radical, OH; and, when a small amount of molecular oxygen is present, the hydroperoxyl radical, HO_2. Laboratory studies have suggested that the recombination of carbon monoxide and atomic oxygen is catalyzed in the presence of these radicals (76). Two recent model calculations incorporate the concepts of transport by eddy diffusion from the upper to the lower atmosphere, where catalytic recombination of atomic oxygen and carbon monoxide takes place (64, 73). The primary sequence of reactions is:

$$H + O_2 + CO_2 \rightarrow HO_2 + CO_2$$
$$HO_2 + O \rightarrow OH + O_2$$
$$OH + CO \rightarrow H + CO_2$$

with the net result of carbon monoxide and atomic oxygen combining to form carbon dioxide

$$CO + O \rightarrow CO_2$$

The results of the two model calculations are shown in Figure 22. Details of the two calculations are not identical; namely, some of the reaction rate coefficients differ, different eddy diffusion coefficients are used, and the mixing ratio of water vapor is different in the two models. However, the major results are similar and the differences illustrate the range of possible results depending on the actual conditions. In the upper part of Figure 22 the density distributions with and without water vapor are shown. In the lowest 10 km of a dry carbon dioxide atmosphere, atomic oxygen is calculated to have a concentration of several parts in one hundred million. (The volume density of the Mars atmosphere at the surface is 2×10^{17} molecules cm^{-3}.) Ozone, formed from atomic and molecular oxygen, is more abundant than atomic oxygen, with a concentration of several parts in ten million. When water vapor is present, the densities of both atomic oxygen and ozone decrease markedly. Figure 22 shows that of the reactive radicals, the density of hydroperoxyl, HO_2, is greater than the density of atomic hydrogen, H, which in turn is greater than the density of the hydroxyl radical, OH. In the model with the larger amount of water vapor, hydrogen peroxide, H_2O_2, is present with a concentration of one part in ten million. Photolysis of H_2O_2 is an important source of OH for the reaction with CO (73). Even at these low concentrations, the cyclic reactions involving H, OH, and HO_2 catalytically recombine CO and O while not being consumed themselves.

These model calculations also illustrate the manner in which the presence of water vapor in the atmosphere inhibits the formation of ozone. In the regions of Mars where the Mariner 9 infrared interferometer spectrometer experiment measured 10–20 μm of precipitable water, the ultraviolet spectrometer determined that the amount of ozone was less than 3 μm-atm (10, 33). In the polar regions, where the infrared experiment measured the atmospheric temperature to be less than

© Annual Reviews Inc. • Provided by the NASA Astrophysics Data System

1974AREPS...2..333B

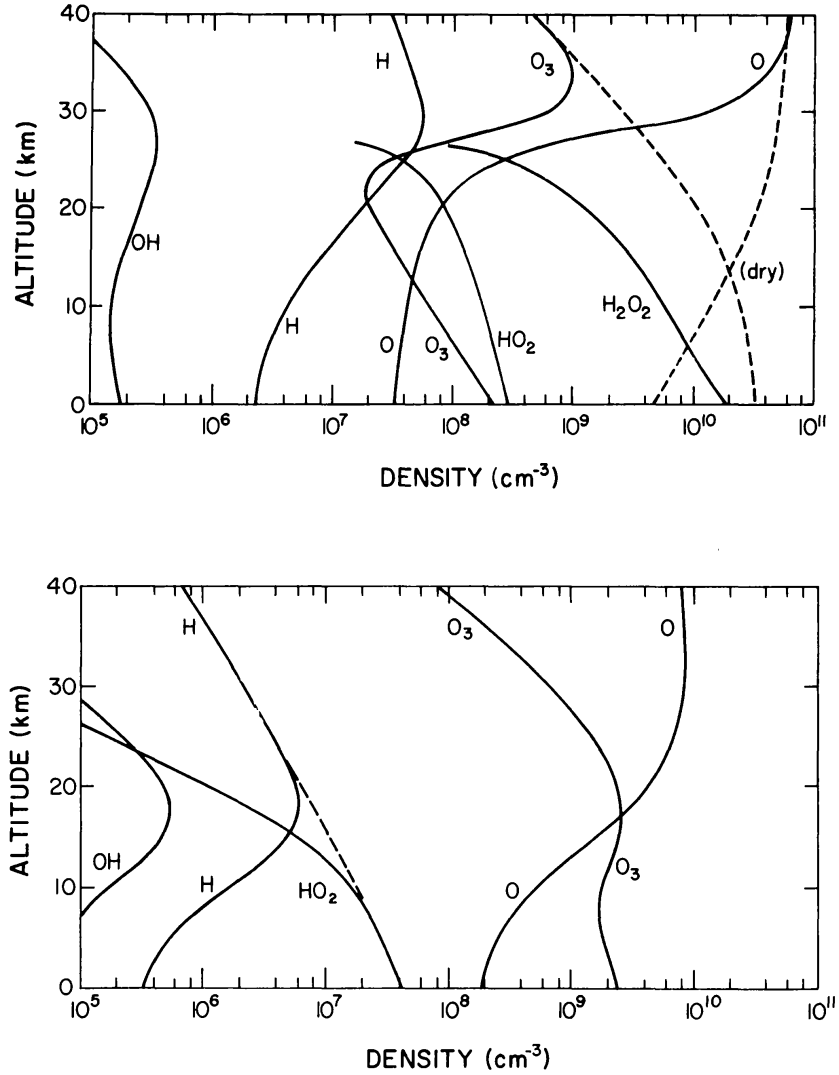

Figure 22 Photochemistry of Mars atmosphere. Density distributions are based on calculations by Parkinson & Hunten (73) (upper figure) and by McElroy & Donahue (64) (lower figure). (Upper Figure reproduced by permission of *J. Atmos. Sci.*; lower figure copyright 1972 by the American Association for the Advancement of Science.)

180°K, the ultraviolet experiment measured ozone in amounts varying between 10 and 60 μm-atm. Since the vapor pressure of water at 180°K is equivalent to 1 μm of precipitable water, the polar atmosphere contains much less than this amount (19). In the upper part of Figure 22, the calculated amount of ozone for the dry atmosphere is approximately 20 μm-atm (73). For atmospheres containing 15 μm of precipitable water, the upper part of the figure shows a calculated amount of ozone equivalent to 0.1 μm-atm (73), while in the lower part of the figure, for the same amount of water vapor, the calculated amount of ozone is approximately 2 μm-atm (64). Both results agree with the ultraviolet observations. It is the

© Annual Reviews Inc. • Provided by the NASA Astrophysics Data System

1974AREPS...2..333B

photodissociation products of water vapor, hydroperoxyl and hydroxyl radicals, and atomic hydrogen, that control the amount of ozone and atomic oxygen, even though their densities are much less than the density of the ozone. The photochemistry occurring in the lower atmosphere of Mars is similar to that which occurs in the stratosphere of the earth.

ATMOSPHERIC ESCAPE

Atomic hydrogen was discovered in the upper atmosphere of Mars in 1969 by the Mariner 6 and 7 ultraviolet spectrometer experiment (6). From the temperature of the upper atmosphere measured by the same experiment (350°K), it was recognized that evaporative escape of atomic hydrogen must occur in the Mars exosphere and that the time constant for escape was approximately 4 hr (7, 9). A radiative transfer analysis of the Mariner 6 Lyman alpha data determined that the density of atomic hydrogen at the bottom of the exosphere (250 km altitude) is 3×10^4 atoms cm^{-3} and that the escape flux is 2×10^8 atoms cm^{-2} sec^{-1} (2). The amount of water vapor observed in the Mars lower atmosphere, 20 μm of precipitable water, is sufficient to supply this amount of atomic hydrogen for 21,000 years.

In 1971, during the first 30 days of Mariner 9 observations, the temperature of the upper atmosphere was somewhat less than in 1969, but the density of atomic hydrogen appeared to be somewhat greater (9). The escape fluxes remained approximately the same as the 1969 Mariner values.

While the photodissociation of water vapor is the most probable ultimate source of hydrogen, it has been suggested that the atomic hydrogen source in the upper atmosphere is an ionospheric reaction between molecular hydrogen and ionized carbon dioxide (61).

$$H_2 + CO_2^+ \rightarrow H + CO_2H^+$$

Molecular hydrogen is produced in the lower atmosphere by the reaction between the water vapor photodissociation products, hydroperoxyl radicals, and atomic hydrogen.

$$HO_2 + H \rightarrow H_2 + O_2$$

It is transported into the ionosphere where it is converted into atomic hydrogen (38). Since the escape flux of atomic hydrogen must be supplied by an upward flux from the chemical production source, any change in the production should be reflected in a change in the escape flux. Since the production of molecular hydrogen is determined by the oxidation state of the atmosphere, the escape of atomic hydrogen from the exosphere is regulated by the amount of atomic oxygen in the Mars atmosphere, although the time constant for this feedback is very long (60). Interestingly, the escape flux of atomic hydrogen, on the two occasions in 1969 measured by Mariner 6 and 7, and during the thirty days in 1971 measured by Mariner 9, remained essentially constant (9). Also, the atomic oxygen density measured by the ultraviolet spectrometer experiments on Mariner 6, 7, and 9 is

© Annual Reviews Inc. • Provided by the NASA Astrophysics Data System

1974AREPS...2..333B

essentially the same in 1969 and in 1971; namely, between 0.5 and 1.0% at the ionization peak (90, 91).

As a consequence of reactions in the Mars ionosphere, atomic oxygen is converted into ionized molecular oxygen, through the reaction with ionized carbon dioxide (87).

$$O + CO_2^+ \rightarrow O_2^+ + CO$$

When either molecular oxygen ions or carbon dioxide ions undergo dissociative recombination, oxygen atoms are produced with excess kinetic energy.

$$O_2^+ + e \rightarrow O + O + \text{excess energy}$$
$$CO_2^+ + e \rightarrow CO + O + \text{excess energy}$$

It has been suggested that many of these "hot" oxygen atoms are able to escape from the low gravitational field of Mars (60). Furthermore, the escape flux of atomic oxygen by this mechanism would balance the escape flux of atomic hydrogen, considering that the dissociation of water vapor is the ultimate source of both atoms in the Mars atmosphere (64).

Other ionospheric reactions can lead to the nonthermal escape of carbon atoms and nitrogen atoms from Mars (60). Dissociative recombination of carbon monoxide ions and molecular nitrogen ions can produce carbon atoms and nitrogen atoms, respectively, with energy greater than the gravitational energy of these atoms in the Mars upper atmosphere.

$$CO^+ + e \rightarrow C + O + \text{excess energy}$$
$$N_2^+ + e \rightarrow N + N + \text{excess energy}$$

However, whether or not nonthermal escape by these reactions is significant in depleting the Mars atmosphere of carbon and nitrogen depends upon the precise composition of the Mars ionosphere. If, for example, the ionized molecular nitrogen is converted into ionized nitric oxide, the nitrogen atoms produced in the dissociative recombination of this ion would not have sufficient energy to escape from the gravitational field of Mars.

$$NO^+ + e \rightarrow N + O$$

INTERACTIONS BETWEEN THE ATMOSPHERE AND THE POLAR CAPS

Observational evidence that the major portions of the polar caps of Mars are composed of frozen carbon dioxide was acquired by the infrared instruments on Mariner 7 (34, 70, 71). Measurements by the infrared radiometer experiment of the southern polar cap in the spring showed the temperature was 148°K, the temperature of subliming carbon dioxide at a pressure of 6.4 mbar (71). Spectra of the polar cap obtained by the infrared spectrometer experiment contained absorption features at 3.0 and 3.3 μ that are attributed to frozen carbon dioxide (34). High resolution earth-based observations of the Mars south polar cap have revealed a number of

© Annual Reviews Inc. • Provided by the NASA Astrophysics Data System

1974AREPS...2..333B

sharp absorption features between 1.2 and 2.4 μ that are identified as solid CO_2 absorption (48a). Observational evidence that carbon dioxide is the principal constituent of the atmosphere and that the polar caps consist of frozen carbon dioxide supports the idea that the current state and evolution of the Mars atmosphere is controlled by the physical state of the polar caps (49). Carbon dioxide sublimes from the cap in the spring-summer hemisphere, and at the same time it is precipitating and forming a polar cap in the fall-winter hemisphere. Model calculations predict that the amount of carbon dioxide precipitated in the polar regions is so great that a seasonal variation in atmospheric pressure will result with maxima occurring just before the solstices and minima near the equinoxes (49). If the minimum temperature on Mars were lower in the past, or future, and all of the carbon dioxide atmosphere condensed, the amount of solid would be equivalent to a layer 10 cm thick if uniformly distributed over the planet. Conversely, at times of higher minimum temperature, the carbon dioxide polar caps would completely sublime away and the atmospheric pressure would increase. It has been estimated that if the remnant north polar cap were 1 km thick, an atmospheric pressure of 1 bar, the sea level pressure on earth, would result from the complete vaporization of the cap (77). Because the triple point pressure of carbon dioxide is 5.1 bars and the triple point temperature 217°K, the thickness of carbon dioxide in the polar cap cannot exceed a few kilometers. At greater depths, the temperature and pressure would be greater than the triple point and the carbon dioxide would liquify and flow away (78).

Mariner 9 obtained television pictures of the north polar cap just after summer solstice (85) and of the south polar cap throughout the summer in that hemisphere (67). One analysis of these observations proposes that there is a large mass of carbon dioxide equal to 2–5 times that of the present atmosphere buried beneath the north polar cap, but not under the south polar cap (68).

While the seasonal waxing and waning of the polar caps plays an important role in controlling the amount of water vapor in the atmosphere, the existence of a permanent polar cap is of great consequence in the evolution of the Mars atmosphere (49). Each fall and winter water vapor condenses out of the atmosphere over the polar regions, forms the clouds of the polar hood, and precipitates onto the polar cap. At colder temperatures, carbon dioxide snow accumulates on the polar cap in an amount far greater than the water snow. In the spring and summer, the reverse sequence takes place. The carbon dioxide sublimes first, followed by the sublimation of water vapor. Water ice may make up a large part of the polar cap remnant. In fact, the interpretation of the Mariner 9 observations of the south polar cap suggests that the summer remnant is made up of water ice (67). If in the past, water was present on the planet in substantial amounts, it may have migrated to the polar cold trap (49).

Certain of the surface erosional channels observed by Mariner 9 (56) are attributed, with varying degrees of certainty, to be evidence of running water in the past history of Mars (54, 57, 65, 82). Bodies of liquid water cannot exist on Mars today because the atmospheric pressure is so close to the triple point pressure of water, 6.105 mbar. If a large amount of liquid water were placed on the surface

© Annual Reviews Inc. • Provided by the NASA Astrophysics Data System

1974AREPS...2..333B

of Mars today, it would either rapidly freeze or vaporize, or do both simultaneously. If in the past, the atmospheric pressure were higher and there were larger amounts of water, then flowing water could have existed (77).

Evidence of climatic variability on Mars is found in the laminated terrain discovered in the polar regions of Mars by Mariner 9 (67). A series of thin layers some tens of meters thick are arranged in plates that are offset one from the other (21). Long term periodic variations in solar radiation reaching the surface have been suggested as producing periodicity in the formation of the layers and plates (69). The growth and recession of the polar caps each year is very sensitive to the amount of insolation that reaches the polar region which, in turn, is determined by the obliquity of Mars (the angle between the spin axis and the normal to the orbit plane). Calculations show that the Mars obliquity could vary from its present value of 25° to as small as 15° and as large as 35° with a 160,000-yr period superimposed on a 1,200,000-yr period (92). These variations are shown in Figure 23. If there were no other changes, at 35° the annual polar insolation would be 35% greater than its present value, while at 15° it would be only 60% of the current value. Variations of this magnitude would produce substantial climatic changes: there is even the possibility of polar cap—atmosphere system instabilities so that dramatic climatic changes could occur as well (79). Calculations of pressure of the Mars atmosphere for different values of insolation show that atmospheric heat transport may make the atmospheric pressure very sensitive to changes in the amount of solar radiation reaching the polar regions (29). Under present conditions, the atmosphere is so thin that heat conduction by the atmosphere is not very effective. However, if the polar insolation increases, carbon dioxide vaporizes, increasing the atmospheric density which makes the atmosphere more effective in transporting heat from the equator to the pole. Increased heating of the pole would vaporize

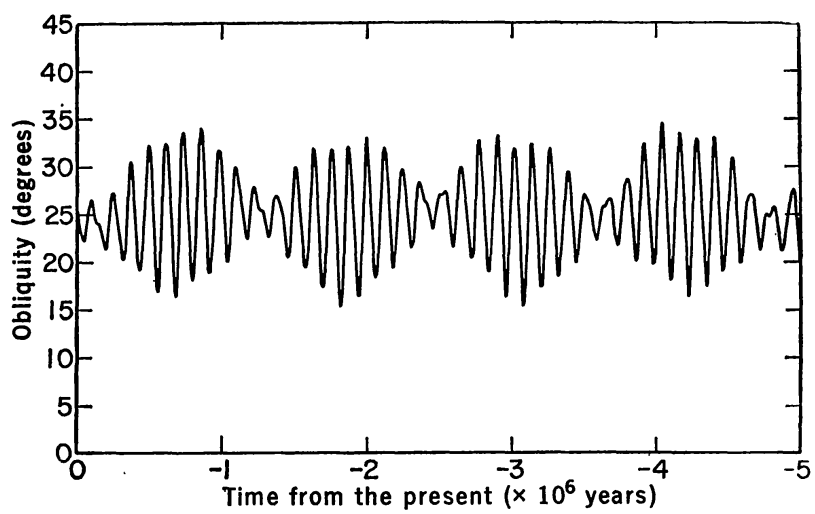

Figure 23 Variations in the obliquity of Mars for the past five million years (92). (Copyright 1973 by the American Association for the Advancement of Science.)

© Annual Reviews Inc. • Provided by the NASA Astrophysics Data System

1974AREPS...2..333B

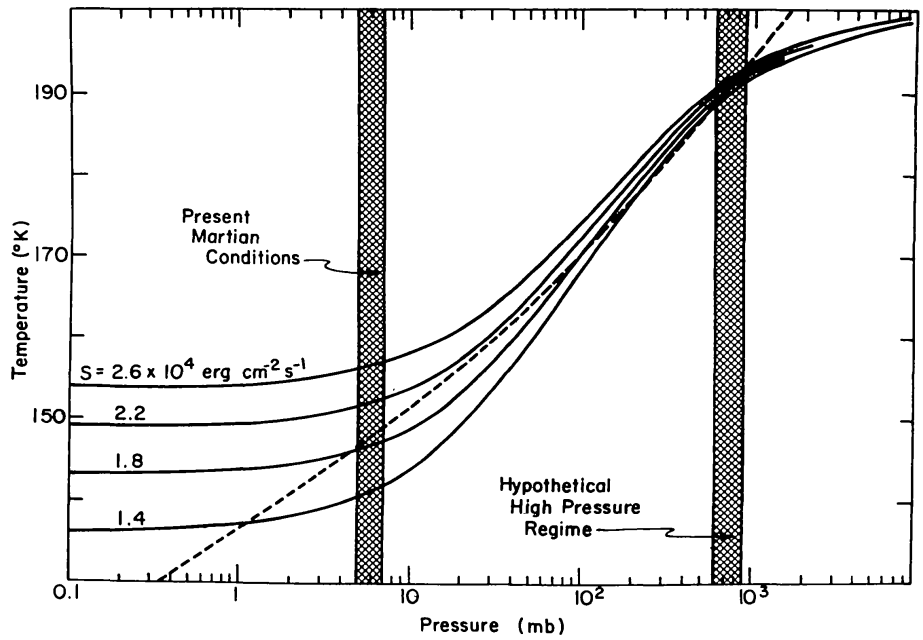

Figure 24 Calculations of Mars polar cap temperature with atmospheric pressure for several values of absorbed solar radiation (79). (Copyright 1973 by the American Association for the Advancement of Science.)

more carbon dioxide and the possibility of a runaway would exist. Figure 24 shows the results of these calculations for a set of conditions that would allow the atmospheric pressure to increase to 1 bar if the polar insolation increased by 14% over its present value (79). If the amount of carbon dioxide in the polar reservoir were not sufficient to produce 1 bar of atmospheric pressure, the pressure increase would stop when all of the carbon dioxide had sublimed. If the temperature of the polar cap continued to increase, then other volatiles, including water could continue to vaporize. A permanent polar cap has been recognized as a cold trap not only for water but for other atmospheric volatiles as well (49).

QUESTIONS STILL TO BE ANSWERED

Our knowledge of the Mars atmosphere has increased vastly during the past several years, but as very often happens, this increased knowledge leads to new questions about the present state of the atmosphere, its history, and origin. Since carbon dioxide is the principal constituent of the atmosphere and since the temperature of the polar cap is sufficiently low to freeze carbon dioxide, a very important question that pertains to both the present state and history of the atmosphere is: "What is the size of the frozen carbon dioxide reservoir at the polar caps?" A related question is: "Is there an annual variation in the amount of carbon dioxide in the atmosphere?" Another important question is: "How much water is stored in the polar caps and how much of it is released and recovered each

© Annual Reviews Inc. • Provided by the NASA Astrophysics Data System

1974AREPS...2..333B

season?" Because of the very low temperature of the polar caps, this same line of inquiry leads to a question whose answer may reveal the history of chemical evolution of the atmosphere: "Are there any other volatiles stored in the polar caps?" Because of the great importance of the role of water vapor in the atmosphere, another question is: "Are there sources of water outgassing from the interior of the planet today?" The intricate interrelationship among water vapor, ozone, and the undissociated character of the carbon dioxide atmosphere leads to a desire to understand better the photochemistry of these constituents and how their abundances vary seasonally and on longer time scales. Even though the temperature and structure of the upper atmosphere was measured several times over a number of years, and then intensively for several months, it is not clear whether or not the basic heating and cooling mechanisms are understood. Without this knowledge, it is difficult to extrapolate our understanding of the evolutionary state of the atmosphere into either the past or future. Observations of the rate of escape of all escaping constituents over several Mars seasons may provide data to allow such extrapolation to be made. Measurement of the amount of nitrogen in the atmosphere to levels below the 1% upper limit set by Mariner observations, and measurement of the rare gas content of the atmosphere, particularly neon and argon, will greatly enhance our knowledge of the history and origin of the atmosphere. The immense problem of understanding the general circulation on Mars needs to be solved, not only for its own sake, but because the circulation plays a very important role in transporting volatiles from one part of the planet to another. As a final question, we return to the first question asked in this section, but stated in a much more general way: "Did Mars have a substantially different climate in the past, and, if so, how and why did it change?"

Acknowledgments

Much of the information and many ideas in this review were acquired from my Mariner 9 experimenter colleagues, both from the published material cited in the references and from personal conversation. Many of the ideas of what are important unanswered questions were developed through interaction with Professor C. B. Leovy of the University of Washington and Professor P. J. Gierasch of Cornell University. Mrs. S. Schaffner and Mrs. R. A. Goettge aided in the preparation of the manuscript. The National Aeronautics and Space Administration sponsored this research activity.

Literature Cited

1. Ajello, J. M., Hord, C. W., Barth, C. A., Stewart, A. I., Lane, A. L. 1973. Afternoon terminator observations of Mars. *J. Geophys. Res.* 78:4279–90
2. Anderson, D. E. Jr., Hord, C. W. 1971. Mariner 6 and 7 ultraviolet spectrometer experiment: Analysis of hydrogen lyman alpha data. *J. Geophys. Res.* 76:6666–73
3. Barker, E. S. 1972. Detection of molecular oxygen in the Martian atmosphere. *Nature* 238:447–48
4. Barker, E. S., Schorn, R. A., Woszczyk, A., Tull, R. G., Little, S. J. 1970. Mars: Detection of atmospheric water vapor during the southern hemisphere spring and summer season. *Science* 170:1308–10
5. Barth, C. A. 1969. Planetary ultraviolet spectroscopy. *Appl. Opt.* 8:1295–304
6. Barth, C. A. et al 1969. Mariner 6: Ultraviolet spectrum of Mars upper atmosphere. *Science* 165:1004–5

© Annual Reviews Inc. • Provided by the NASA Astrophysics Data System

1974AREPS...2..333B

7. Barth, C. A. et al 1971. Mariner 6 and 7 ultraviolet spectrometer experiment: Upper atmosphere data. *J. Geophys. Res.* 76:2213–27
8. Barth, C. A., Hord, C. W. 1971. Mariner ultraviolet spectrometer: Topography and polar cap. *Science* 173: 197–201
9. Barth, C. A., Stewart, A. I., Hord, C. W., Lane, A. L. 1972. Mariner 9 ultraviolet spectrometer experiment: Mars airglow spectroscopy and variations in Lyman alpha. *Icarus* 17:457–68
10. Barth, C. A. et al 1973. Mariner 9 ultraviolet spectrometer experiment: Seasonal variation of ozone on Mars. *Science* 179:795–96
11. Barth, C. A., Dick, M. L. Ozone and the polar hood of Mars. *Icarus.* Submitted for publication
12. Baum, W. A., Martin, L. J. 1973. Behavior of the Martian polar caps since 1905. *Bull. Am. Astron. Soc.* 5:296
13. Beer, R., Norton, R. H., Martonchik, J. V. 1971. Astronomical infrared spectroscopy with a Connes-type interferometer: II—Mars, 2500–3500 cm^{-1}. *Icarus* 15:1–10
14. Belton, M. J. S., Broadfoot, A. L., Hunten, D. M. 1968. Abundance and temperature of CO_2 on Mars during the 1967 opposition. *J. Geophys. Res.* 73: 4795–806
15. Blumsack, S. L., Gierasch, P. J. 1973. The vertical thermal structure of the Martian atmosphere: Modification by motions. *Icarus* 18:126–33
16. Capen, C. F., Martin, L. J. 1972. Mars' great storm of 1971. *Sky Telesc.* 43: 276–79
17. Carleton, N. P., Traub, W. A. 1972. Detection of molecular oxygen on Mars. *Science* 177:988–92
18. Connes, J., Connes, P., Maillard, J. P. 1969. *Atlas des spectres infrarouges de Venus, Mars, Jupiter et Saturne.* Paris: Editions Centre National Recherche Scientifique
19. Conrath, B. et al 1973. Atmospheric and surface properties of Mars obtained by infrared spectroscopy on Mariner 9. *J. Geophys. Res.* 78:4267–78
20. Curran, R. J., Conrath, B. J., Hanel, R. A., Kunde, V. G., Pearl, J. C. 1973. Mars: Mariner 9 spectroscopic evidence for H_2O ice clouds. *Science* 182:381–83
21. Cutts, J. A. 1973. Nature and origin of layered deposits of the Martian polar regions. *J. Geophys. Res.* 78:4231–49
22. Dalgarno, A., McElroy, M. B. 1970. Mars: Is nitrogen present? *Science* 170:167–68
23. Dementyeva, N. N., Kurt, V. G., Smirnov, A. S., Titarchuk, L. G., Chuvahin, S. D. 1972. Preliminary results of measurements of uv emissions scattered in the Martian upper atmosphere. *Icarus* 17:475–83
24. Fehsenfeld, F. C., Dunkin, D. B., Ferguson, E. E. 1970. Rate constants for the reaction of CO_2^+ with O, O_2 and NO; N_2^+ with O and NO; and O_2^+ with NO. *Planet. Space Sci.* 18: 1267–69
25. Fjeldbo, G., Eshleman, V. R. 1968. The atmosphere of Mars analyzed by integral inversion of the Mariner IV occultation data. *Planet. Space Sci.* 16: 1035–59
26. Fjeldbo, G., Kliore, A., Seidel, B. 1970. The Mariner 1969 occultation measurements of the upper atmosphere of Mars. *Radio Sci.* 5:381–86
27. Gierasch, P., Goody, R. 1968. A study of the thermal and dynamical structure of the Martian lower atmosphere. *Planet. Space Sci.* 16:615–46

27a. Gierasch, P. J., Sagan, C. 1971. A preliminary assessment of Martian wind regimes. *Icarus* 14:312–18

28. Gierasch, P. J., Goody, R. M. 1972. The effect of dust on the temperature of the Martian atmosphere. *J. Atmos. Sci.* 29: 400–2
29. Gierasch, P. J., Toon, O. B. 1973. Atmospheric pressure variation and the climate of Mars. *J. Atmos. Sci* 8:1502–8
30. Gierasch, P. J., Goody, R. M. 1973. A model of a Martian great dust storm. *J. Atmos. Sci.* 30:169–79
31. Golitsyn, G. S. 1973. On the Martian dust storm. *Icarus* 18:113–19
32. Hanel, R. A. et al 1972. Infrared spectroscopy experiment on the Mariner 9 mission: Preliminary results. *Science* 175:305–8
33. Hanel, R. et al 1972. Investigation of the Martian environment by infrared spectroscopy on Mariner 9. *Icarus* 17: 423–42
34. Herr, K. C., Pimentel, G. C. 1969. Infrared absorptions near three microns recorded over the polar cap of Mars. *Science* 166:496–99

34a. Herr, K. C., Pimentel, G. C. 1970. Evidence for solid carbon dioxide in the upper atmosphere of Mars. *Science* 167: 47–49

35. Hord, C. W., Barth, C. A., Stewart, A. I., Lane, A. L. 1972. Mariner 9 ultraviolet spectrometer experiment: Photometry and topography of Mars. *Icarus* 17:443–56
36. Hord, C. W., Simmons, K. E.,

© Annual Reviews Inc. • Provided by the NASA Astrophysics Data System

1974AREPS...2..333B

McLaughlin, L. K. 1974. Mariner 9 ultraviolet spectrometer experiment: Pressure altitude measurements on Mars. *Icarus*. In press
37. Horn, D., McAfee, J. M., Winer, A. M., Herr, K. C., Pimentel, G. C. 1972. The composition of the Martian atmosphere: Minor constituents. *Icarus* 16:543–56
38. Hunten, D. M., McElroy, M. B. 1970. Production and escape of hydrogen on Mars. *J. Geophys. Res.* 75:5989–6001
39. Kaplan, L. D., Connes, J., Connes, P. 1969. Carbon monoxide in the Martian atmosphere. *Ap. J.* 157:L187–92
40. Kieffer, H. H., Chase, S. C., Miner, E., Münch, G., Neugebauer, G. 1973. Preliminary report on infrared radiometric measurements from the Mariner 9 spacecraft. *J. Geophys. Res.* 78:4291–4312
41. Kliore, A. et al 1965. Occultation experiment: Results of the first direct measurement of Mars' atmosphere and ionosphere. *Science* 149:1243–48
42. Kliore, A., Fjeldbo, G., Seidel, B. L., Rasool, S. I. 1969. Mariners 6 and 7: Radio occultation measurements of the atmosphere of Mars. *Science* 166:1393–97
43. Kliore, A. J., Fjeldbo, G., Seidel, B. L. 1971. Summary of Mariner 6 and 7 radio occultation results on the atmosphere of Mars. *Space Res.* XI:165–75
44. Kliore, A. J., Cain, D. L., Fjeldbo, G., Seidel, B. L., Rasool, S. I. 1972. Mariner 9 S-band Martian occultation experiment: Initial results on the atmosphere and topography of Mars. *Science* 175:313–17
45. Kliore, A. J. et al 1972. The atmosphere of Mars from Mariner 9 radio occultation measurements. *Icarus* 17:484–516
46. Kliore, A. J., Fjeldbo, G., Seidel, B. L., Sykes, M. J., Woiceshyn, P. M. 1973. S-band radio occultation measurements of the atmosphere and topography of Mars with Mariner 9: Extended mission coverage of polar and intermediate latitudes. *J. Geophys. Res.* 78:4331–51
47. Kurt, V. G., Smirnov, A. S., Titarchuk, L. G., Chuvahin, S. D. 1974. Observation of scattered radiation in the OI triplet lines at 1300 Å in the Martian atmosphere. *Icarus*. 21:35–41
48. Lane, A. L., Barth, C. A., Hord, C. W., Stewart, A. I. 1973. Mariner 9 ultraviolet spectrometer experiment: Observations of ozone on Mars. *Icarus* 18:102–8
48a. Larson, H. P., Fink, U. 1972. Identification of carbon dioxide frost on the Martian polar caps. *Science* 153:136–44
49. Leighton, R. B., Murray, B. C. 1966. Behavior of carbon dioxide and other volatiles on Mars. *Science* 153:136–44
49a. Leovy, C. B., Mintz, Y. 1969. Numerical simulation of the atmospheric circulation and climate of Mars. *J. Atmos. Sci.* 26:1167–90
50. Leovy, C. B. et al 1972. The Martian atmosphere: Mariner 9 television experiment progress report. *Icarus* 17:373–93
51. Leovy, C. B. 1973. Exchange of water vapor between the atmosphere and surface of Mars. *Icarus* 18:120–25
52. Leovy, C. B., Briggs, G. A., Smith, B. A. 1973. Mars atmosphere during the Mariner 9 extended mission: Television results. *J. Geophys. Res.* 78:4252–66
53. Leovy, C. B., Zurek, R. W., Pollack, J. B. 1973. Mechanisms for Mars dust storms. *J. Atmos. Sci.* 30:749–62
54. Masursky, H. 1973. An overview of geological results from Mariner 9. *J. Geophys. Res.* 78:4009–30
55. Masursky, H. et al 1972. Mariner 9 television reconnaissance of Mars and its satellites: Preliminary results. *Science* 175:294–304
56. McCauley, J. F. et al 1972. Preliminary Mariner 9 report on the geology of Mars. *Icarus* 17:289–327
57. McCauley, J. F. 1973. Mariner 9 evidence for wind erosion in the equatorial and mid-latitude regions of Mars. *J. Geophys. Res.* 78:4123–37
58. McElroy, M. B. 1967. The upper atmosphere of Mars. *Ap. J.* 150:1125–38
59. McElroy, M. B. 1969. Structure of the Venus and Mars atmospheres. *J. Geophys. Res.* 74:29–41
60. McElroy, M. B. 1972. Mars: An evolving atmosphere. *Science* 175:443–45
61. McElroy, M. B., Hunten, D. M. 1969. Molecular hydrogen in the atmosphere of Mars. *J. Geophys. Res.* 74:5807–9
62. McElroy, M. B., Hunten, D. M. 1970. Photochemistry of CO_2 in the atmosphere of Mars. *J. Geophys. Res.* 75:1188–201
63. McElroy, M. B., McConnell, J. C. 1971. Dissociation of CO_2 in the Martian atmosphere. *J. Atmos. Sci.* 28:879–84
64. McElroy, M. B., Donahue, T. M. 1972. Stability of the Martian atmosphere. *Science* 177:986–88
65. Milton, D. J. 1973. Water and processes of degradation in the Martian landscape. *J. Geophys. Res.* 78:4037–47
66. Moroz, V. I., Ksanfomaliti, L. V. 1972. Preliminary results of astrophysical

© Annual Reviews Inc. • Provided by the NASA Astrophysics Data System

1974AREPS...2..333B

observations of Mars from Mars-3. *Icarus* 17:408–22
67. Murray, B. C. et al 1972. Geological framework of the south polar region of Mars. *Icarus* 17:328–45
68. Murray, B. C., Malin, M. C. 1973. Polar volatiles on Mars—Theory versus observation. *Science* 182:437–43
69. Murray, B. C., Ward, W. R., Yeung, S. C. 1973. Periodic insolation variations on Mars. *Science* 180:638–40
70. Neugebauer, G. et al 1969. Mariner 1969: Preliminary results of the infrared radiometer experiment. *Science* 166: 98–99
71. Neugebauer, G., Münch, G., Kieffer, H., Chase, S. C. Jr., Miner, E. 1971. Mariner 1969 infrared radiometer results: Temperature and thermal properties of the Martian surface. *Ap. J.* 76:719–28
72. Owen, T., Sagan, C. 1972. Minor constituents in planetary atmospheres: Ultraviolet spectroscopy from the orbiting astronomical observatory. *Icarus* 16:557–68
73. Parkinson, T. D., Hunten, D. M. 1972. Spectroscopy and aeronomy of O_2 on Mars. *J. Atmos. Sci.* 29:1380–90
74. Peale, S. J. 1973. Water and the Martian W cloud. *Icarus* 18:497–501
75. Rasool, S. I., Hogan, J. S., Stewart, R. W., Russell, L. H. 1970. Temperature distributions in the lower atmosphere of Mars from Mariner 6 and 7 radio occultation data. *J. Atmos. Sci.* 27: 841–43
76. Reeves, R. R. Jr., Harteck, P., Thompson, B. A., Waldron, R. W. 1966. Photochemical equilibrium studies of carbon dioxide and their significance for the Venus atmosphere. *J. Phys. Chem.* 70: 1637–40
77. Sagan, C. 1971. The long winter model of Martian biology: A speculation. *Icarus* 15:511–14
78. Sagan, C. 1973. Liquid carbon dioxide and the Martian polar laminae. *J. Geophys. Res.* 78:4250–51
79. Sagan, C., Toon, O. B., Gierasch, P. J. 1973. Climatic change on Mars. *Science* 181:1045–49
80. Sagan, C. et al 1973. Variable features on Mars, 2: Mariner 9 global results. *J. Geophys. Res.* 78:4163–96
81. Schorn, R. A., Spinrad, H., Moore, R. C., Smith, H. J., Giver, L. P. 1967. High-dispersion spectroscopic observations of Mars II. The water-vapor variations. *Ap. J.* 147:743–52
82. Sharp, R. P. 1973. Mars: Troughed terrain. *J. Geophys. Res.* 78:4063–72
83. Shimizu, M. 1968. The recombination mechanism of CO and O in the upper atmospheres of Venus and Mars. *Icarus* 9:593–97
84. Smith, S. A., Smith, B. A. 1972. Diurnal and seasonal behavior of discrete white clouds on Mars. *Icarus* 16:509–21
85. Soderblom, L. A., Malin, M. C., Cutts, J. A., Murray, B. C. 1973. Mariner 9 observations of the surface of Mars in the north polar region. *J. Geophys. Res.* 78:4197–210
86. Spinrad, H., Münch, G., Kaplan, L. D. 1963. The detection of water vapor on Mars. *Ap. J.* 137:1319–21
87. Stewart, A. I. 1972. Mariner 6 and 7 ultraviolet spectrometer experiment: Implications of CO_2^+, CO, and O airglow. *J. Geophys. Res.* 77:54–68
88. Stewart, A. I., Barth, C. A., Hord, C. W., Lane, A. L. 1972. Mariner 9 ultraviolet spectrometer experiment: Structure of Mars' upper atmosphere. *Icarus* 17:469–74
89. Stone, P. H. 1972. A simplified radiative-dynamical model for the static stability of rotating atmospheres. *J. Atmos. Sci.* 29:405–18
90. Strickland, D. J., Thomas, G. E., Sparks, P. R. 1972. Mariner 6 and 7 ultraviolet spectrometer experiment: Analysis of the O I 1304- and 1356-Å emissions. *J. Geophys. Res.* 77:4052–68
91. Strickland, D. J., Stewart, A. I., Barth, C. A., Hord, C. W., Lane, A. L. 1973. Mars atomic oxygen 1304 Å emission. *J. Geophys. Res.* 78:4547–59
92. Ward, W. R. 1973. Large-scale variations in the obliquity of Mars. *Science* 181: 260–62
93. Young, L. D. G. 1969. Interpretation of high-resolution spectra of Mars I. CO_2 abundance and surface pressure derived from the curve of growth. *Icarus* 11: 386–89
94. Young, L. D. G. 1971. Interpretation of high resolution spectra of Mars-III. Calculations of CO abundance and rotational temperature. *J. Quant. Spectrosc. Radiat. Transfer* 11:385–90

© Annual Reviews Inc. • Provided by the NASA Astrophysics Data System